Econometric Theory, **31**, 2015, 981–1015.
doi:10.1017/S0266466614000607

HIDDEN MARKOV STRUCTURES FOR DYNAMIC COPULAE

WOLFGANG KARL HÄRDLE, OSTAP OKHRIN, AND WEINING WANG
Humboldt-Universität zu Berlin

Understanding the time series dynamics of a multi-dimensional dependency structure is a challenging task. Multivariate covariance driven Gaussian or mixed normal time varying models have only a limited ability to capture important features of the data such as heavy tails, asymmetry, and nonlinear dependencies. The present paper tackles this problem by proposing and analyzing a hidden Markov model (HMM) for hierarchical Archimedean copulae (HAC). The HAC constitute a wide class of models for multi-dimensional dependencies, and HMM is a statistical technique for describing regime switching dynamics. HMM applied to HAC flexibly models multivariate dimensional non-Gaussian time series.

We apply the expectation maximization (EM) algorithm for parameter estimation. Consistency results for both parameters and HAC structures are established in an HMM framework. The model is calibrated to exchange rate data with a VaR application. This example is motivated by a local adaptive analysis that yields a time varying HAC model. We compare its forecasting performance with that of other classical dynamic models. In another, second, application, we model a rainfall process. This task is of particular theoretical and practical interest because of the specific structure and required untypical treatment of precipitation data.

1. INTRODUCTION

Modeling multi-dimensional time series is often an underestimated exercise of routine econometrical and statistical work. This slightly pejorative attitude towards day to day statistical analysis is unjustified since actually the calibration of time series models in several dimensions for standard data sizes is not only difficult on the numerical side but also on the mathematical side. Computationally speaking, integrated models for multi-dimensional time series become more involved when the parameter space is too large. Consequently the mathematical and econometrical aspects become more difficult since the parameter space becomes too complex, especially when their time variation is allowed. An example is the multivariate GARCH(1,1) BEKK model, which for even two dimensions

Our special thanks go to Oliver Linton, Peter Phillips, Cheng-Der Fuh and referees for helpful comments. We remain responsible for errors and omission.
The financial support from the Deutsche Forschungsgemeinschaft via SFB 649 "Ökonomisches Risiko", Humboldt-Universität zu Berlin and IRTG 1972 "High Dimensional Non Stationary Time Series" is gratefully acknowledged.
Address correspondence to Weining Wang, Hermann-Otto-Hirschfeld Junior Professor in Nonparametric Statistics and Dynamic Risk Management at the Ladislaus von Bortkiewicz Chair of Statistics of Humboldt-Universität zu Berlin, Spandauer Straße 1, 10178 Berlin, Germany; e-mail: wangwein@cms.hu-berlin.de.

has an associated parameter space of dimension 12. For moderate sample sizes, the parameter space dimension might be in the range of the sample size or even bigger. This data situation has evoked a new strand of the literature on dimension reduction via penalty methods.

In this paper we take a different route, by calibrating an integrated dynamic model with unknown dependency structure among the d-dimensional time series variables. More precisely, the unknown dependency structure may vary within a set of given dependencies. These dependency structures might have been selected via a preliminary study, as described in, e.g., Härdle, Herwartz, and Spokoiny (2003). The specific dependence at each time t is unknown to the data analyst, and depends on the dependency pattern at time $t-1$. Therefore, hidden Markov models (HMM) naturally come into play. This leaves us with the task of specifying the set of dependencies.

An approach based on assuming a multivariate Gaussian or mixed normals is inappropriate in the presence of important types of data features such as heavy tails, asymmetry, and nonlinear dependencies. Such a simplification is certainly in practical questions concerning too restrictive tails and might lead to biased results. The use of copulae is one possible approach to solving these problems. Moreover, copulae allow us to separate the marginal distributions and the dependency model, see Sklar (1959). In recent decades, copula-based models have gained popularity in various fields like finance, insurance, biology, hydrology, etc. Nevertheless, many basic multivariate copulae are still too restrictive and the extension to more parameters leads initially to a nonparametric density estimation problem that suffers of course from the curse of dimensionality. A natural compromise is the class of hierarchical Archimedean copulae (HAC). An HAC allows a rich copula structure with a finite number of parameters. Recent research has demonstrated their flexibility (see McNeil and Nešlehová, 2009; Okhrin, Okhrin, and Schmid, 2013; Whelan, 2004).

Insights into the dynamics of copulae have been offered by Chen and Fan (2005), who assume an underlying Markovian structure, and a specific class of copulae functions for the temporal dependence; Patton (2004) considers an asset-allocation problem with a time-varying parameter of bivariate copulae; and Rodriguez (2007) studies financial contagion using switching-parameter bivariate copulae. Similarly, Okimoto (2008) provides strong empirical evidence that a Markov switching multivariate normal model is not appropriate for the dependence structures in international equity markets.

Moreover, an adaptive method isolating a time varying dependency structure via a local change point method (LCP) has been proposed in Giacomini, Härdle, and Spokoiny (2009) and Härdle, Okhrin, and Okhrin (2013). Figure 1 presents an analysis of HAC for exchange rate data using LCP on a moving window, where the window sizes are adaptively selected by the LCP algorithm. It plots the changes of estimated structure (upper panel) and parameters (lower panel) in each window over time. In particular, in the upper panel, the y-axis corresponds to the dependency structures picked by estimation of three-dimensional copulae; in the

https://doi.org/10.1017/S0266466614000607 Published online by Cambridge University Press

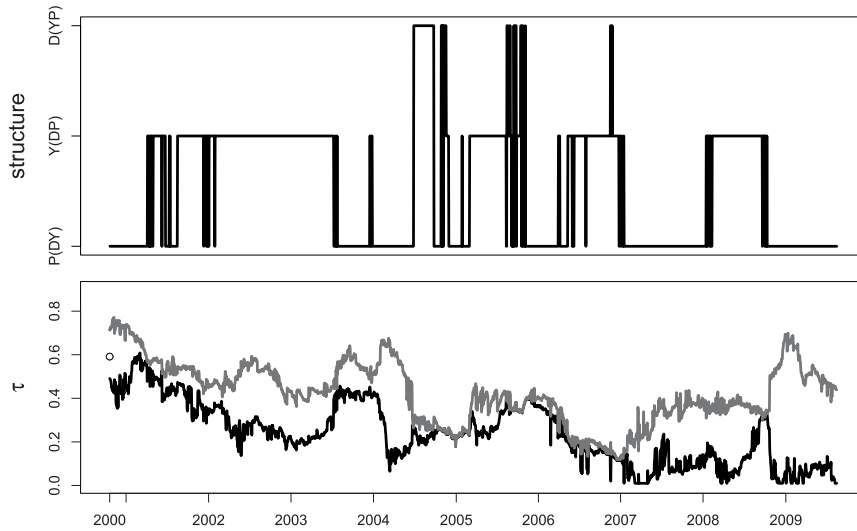

FIGURE 1. LCP for exchange rates: structure (upper) and parameters (lower, θ_1(gray) and θ_2(black)) for Gumbel HAC. $m_0 = 40$ (starting value for the window size in the algorithm).

lower panel, the y-axis shows the two estimated dependency parameters (value converted to Kendall's τ) corresponding to the estimated structure. In more detail, we have three exchange rates series: P (GBP/EUR), Y(JPY/EUR), D(USD/EUR); the label P(DY) means that the pair D and Y have a stronger dependency than other possible pairs. For a more detailed introduction to HAC and their structures, see Section 2.1. One observes that the structure very often remains the same for a long time, the parameters only varying slowly over time. This indicates that the dynamics of HAC functions is likely to be driven by a Markovian sequence seemingly determining the structures and parameter values. This observation motivates us to pursue a different path of modeling the dynamics. Instead of taking a local point of view, we adopt a global dynamic model HMM for the change of both the tree structure and the parameters of the HAC over time. In this situation, the not directly observable underlying Markov process X determines the state of distributions of Y.

HMM has been widely applied to speech recognition, see Rabiner (1989), molecular biology, and digital communications over unknown channels. Markov switching models were introduced to the economics literature by Hamilton (1989), where the trend component of a univariate nonstationary time series changes according to an underlying Markov chain. Later, it was extended and combined with many different time series models, see, e.g., Pelletier (2006). For estimation and inference issues in HMM, see Bickel, Ritov, and Rydén (1998) and Fuh (2003), among others.

In this paper, we propose a new type of dynamic model, called HMM HAC, which incorporates HAC into an HMM framework. The theoretical problems,

https://doi.org/10.1017/S0266466614000607 Published online by Cambridge University Press

such as parameter consistency and structure consistency, are solved. The expectation maximization (EM) algorithm is developed in this framework for parameter estimation. See Section 2 for a description of the model, and Section 3 for theorems about its consistency and asymptotic normality. Issues as to the EM algorithm and computation are in Section 4. Section 5 treats a simulation study, and Section 6 is the applications. The technical details are put into the Appendix.

2. MODEL DESCRIPTION

In this section, we introduce our model and estimation method. Section 2.1 briefly introduces the definition and properties of HAC, and Section 2.2 introduces the HMM HAC. In the last subsection, we describe the estimation and algorithm we use.

2.1. Copulae

Let $Z_1, \ldots, Z_d$ be r.v. with continuous cumulative distribution function (cdf) $F(\cdot)$. The Sklar theorem guarantees the existence and uniqueness of copula functions:

THEOREM 2.1 (Sklar's theorem). *Let F be a multivariate distribution function with margins $F_1^{\mathfrak{m}}, \ldots, F_d^{\mathfrak{m}}$, then a copula C exists such that*

$$F(z_1, \ldots, z_d) = C\{F_1^{\mathfrak{m}}(z_1), \ldots, F_d^{\mathfrak{m}}(z_d)\}, \quad z_1, \ldots, z_d \in \mathbb{R}.$$

If $F_i^{\mathfrak{m}}(\cdot)$ are continuous for $i = 1, \ldots, d$ then $C(\cdot)$ is unique. Otherwise $C(\cdot)$ is uniquely determined on $F_1^{\mathfrak{m}}(\mathbb{R}) \times \cdots \times F_d^{\mathfrak{m}}(\mathbb{R})$.

Conversely, if $C(\cdot)$ is a copula and $F_1^{\mathfrak{m}}, \ldots, F_d^{\mathfrak{m}}$ are univariate distribution functions, then the function F defined above is a multivariate distribution function with margins $F_1^{\mathfrak{m}}, \ldots, F_d^{\mathfrak{m}}$.

The family of Archimedean copulae is very flexible: it captures tail dependency, has an explicit form, and is simple to estimate,

$$C(u_1, \ldots, u_d) = \phi\{\phi^{-1}(u_1) + \cdots + \phi^{-1}(u_d)\}, \quad u_1, \ldots, u_d \in [0, 1], \tag{1}$$

where $\phi(\cdot)$ is defined as the generator of the copula and depends on a parameter θ, see Nelsen (2006). $\phi(\cdot)$ is d monotone, and $\phi(\cdot) \in \mathfrak{L} = \{\phi(\cdot) : [0; \infty) \to (0, 1] \,|\, \phi(0) = 1, \phi(\infty) = 0; (-1)^j \phi^{(j)} \geq 0; \ j = 1, \ldots, d-2\}$. As an example, the Gumbel generator is given by $\phi(x) = \exp(-x^{1/\theta})$ for $0 \leq x < \infty, \ 1 \leq \theta < \infty$.

In the present paper we consider less restrictive compositions of simple Archimedean copulae leading to a Hierarchical Archimedean Copula (HAC) $C(u_1, \ldots, u_d; \boldsymbol{\theta}, s)$, where $s = \{(\ldots(i_1 \ldots i_{j_1}) \ldots (\ldots) \ldots)\}$ denotes the structure of HAC, with $i_\ell \in \{1, \ldots, d\}$ being a reordering of the indices of the variables and s_j the structure of the subcopulae with $s_d = s$, and $\boldsymbol{\theta}$ is the set of copula parameters.

https://doi.org/10.1017/S0266466614000607 Published online by Cambridge University Press

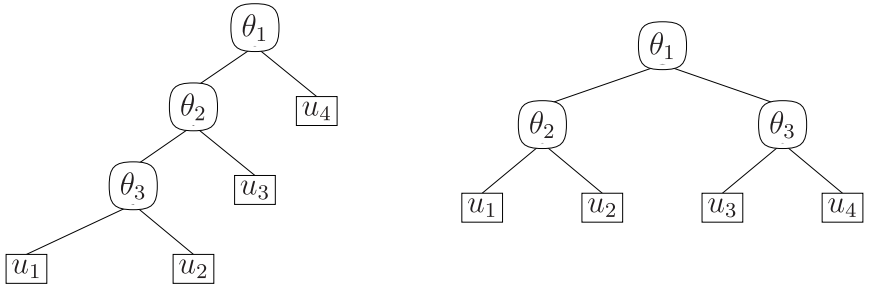

FIGURE 2. Fully and partially nested copulae of dimension $d = 4$ with structures $s = (((12)3)4)$ on the left and $s = ((12)(34))$ on the right.

For example, the fully nested HAC (see Figure 2, left) can be expressed by

$$\begin{aligned} &C(u_1, \ldots, u_d; \boldsymbol{\theta}, s = s_d) \\ &\quad = C\{u_1, \ldots, u_d; (\theta_1, \ldots, \theta_{d-1})^\top, ((s_{d-1})d)\} \\ &\quad = \phi_{d-1,\theta_{d-1}} \Big(\phi^{-1}_{d-1,\theta_{d-1}} \circ C \left\{ u_1, \ldots, u_{d-1}; (\theta_1, \ldots, \theta_{d-2})^\top, ((s_{d-2})(d-1)) \right\} \\ &\qquad\qquad + \phi^{-1}_{d-1,\theta_{d-1}}(u_d) \Big), \end{aligned}$$

where $s = \{(\ldots(12)3)\ldots)d)\}$. On the RHS of Figure 2 we have the partially nested HAC with $s = ((12)(34))$ in dimension $d = 4$.

For more details about HAC, see Joe (1997), Whelan (2004), Savu and Trede (2010), and Okhrin, Okhrin, and Schmid (2013).

It is worth noting that not all generator functions can be mixed within one HAC. We therefore concentrate on one single generator family within one HAC. This boils down to binary structures, i.e., at each level of the hierarchy only two variables are joined together. In fact, this makes the architecture very flexible and yet parsimonious.

Note that not only are the parameters unknown for each HMM HAC, but also the structure has to be determined. We adopt the modified computational steps of Okhrin et al. (2013) to estimate the HAC structure and parameters. One estimates the marginal distributions either parametrically or nonparametrically. Then (assuming that the marginal distributions are known) one selects the couple of variables with the strongest fit and denotes the corresponding estimator of the parameter at the first level by $\hat{\theta}_1$ and the set of indices of the variables by I_1. The selected couple is joined together to define the pseudo-variables $z_1 = C\{(I_1); \hat{\theta}_1, \phi_1\}$. Next, one proceeds in the same way by considering the remaining variables and the new pseudovariable. At every level, the copula parameter is estimated by assuming that the margins as well as the copula parameters at lower levels are known. This algorithm allows us to determine the estimated structure of the copula recursively.

https://doi.org/10.1017/S0266466614000607 Published online by Cambridge University Press

2.2. Incorporating HAC into HMM

A hidden Markov model is a parameterized time series model with an underlying Markov chain viewed as missing data, as in Leroux (1992), Bickel et al. (1998), and Gao and Song (2011). More specifically, in the HMM HAC framework, let $\{X_t, t \geq 0\}$ be a stationary Markov chain of order one on a finite state space $D = \{1, 2, \ldots, M\}$, with transition probability matrix $P = \{p_{ij}\}_{i,j=1,\ldots,M}$ and initial distribution $\pi = \{\pi_i\}_{i=1,\ldots,M}$.

$$\mathrm{P}(X_0 = i) = \pi_i, \tag{2}$$

$$\begin{aligned}\mathrm{P}(X_t = j | X_{t-1} = i) &= p_{ij} \\ &= \mathrm{P}(X_t = j | X_{t-1} = i, X_{t-2} = x_{t-2}, \ldots, X_1 = x_1, X_0 = x_0), \\ &\quad i, j = 1, \ldots, M\end{aligned} \tag{3}$$

Let $\{Y_t, t \geq 0\}$ be the associated observations, and they are adjoined with $\{X_t, t \geq 0\}$ in such a way that given $X_t = i, i = 1, \ldots, M$, the distribution of Y_t is fixed:

$$(X_t | X_{0:(t-1)}, Y_{0:(t-1)}) \overset{\mathcal{L}}{=} (X_t | X_{t-1}), \tag{4}$$

$$(Y_t | Y_{0:(t-1)}, X_{(0:t)}) \overset{\mathcal{L}}{=} (Y_t | X_t), \tag{5}$$

where $Y_{0:(t-1)}$ stands for $\{Y_0, \ldots, Y_{t-1}\}, t < T$.

Let $f_j\{\cdot\}$ be the conditional density of Y_t given $X_t = j$ with $\boldsymbol{\theta} \in \Theta, \mathbf{s} \in S, j = 1, \ldots, M$ being the unknown parameters. Here, $\{X_t, t \geq 0\}$ is the Markov chain, and given $X_0, X_1, \ldots, X_T$, the $Y_0, Y_1, \ldots, Y_T$ are independent. Note that $\boldsymbol{\theta} = (\boldsymbol{\theta}^{(1)}, \ldots, \boldsymbol{\theta}^{(M)}) \in \mathbb{R}^{(d-1)M}$ are the unknown dependency parameters, $\mathbf{s} = (s^{(1)}, \ldots, s^{(M)})$ are the unknown HAC structures. Denote their true values by $\boldsymbol{\theta}^*$ and $\mathbf{s}^*$ respectively.

For the time series $y_1, \ldots, y_T \in \mathbb{R}^d$ ($y_t = (y_{1t}, y_{2t}, y_{3t}, \ldots, y_{dt})^\top$) and the unobservable (or missing) $x_1, \ldots, x_T$ from the given hidden Markov model, define π_{x_0} as the π_i for $x_0 = i, i = 1, \ldots, M$, and $p_{x_{t-1}x_t} = p_{ji}$ for $x_{t-1} = j$ and $x_t = i$. The full likelihood for $\{x_t, y_t\}_{t=1}^T$ is then:

$$p_T(y_{0:T}; x_{0:T}) = \pi_{x_0} f_{x_0}(y_0) \prod_{t=1}^{T} p_{x_{t-1}x_t} f_{x_t}(y_t), \tag{6}$$

and the likelihood for the observations $\{y_t\}_{t=1}^T$, only is calculated by marginalization:

$$p_T(y_{0:T}) = \sum_{x_0=1}^{M} \cdots \sum_{x_T=1}^{M} \pi_{x_0} f_{x_0}(y_0) \prod_{t=1}^{T} p_{x_{t-1}x_t} f_{x_t}(y_t). \tag{7}$$

The HAC is a parameterization of $f_{x_t}(y_t)(x_t = i)$, which helps properly understand the dynamics of a multivariate distribution. Up to now, typical parameterizations have been mixtures of log-concave or elliptical symmetric densities,

https://doi.org/10.1017/S0266466614000607 Published online by Cambridge University Press

such as those from Gamma or Poisson families, which are not flexible enough to model multi-dimensional time series. The advantage of the copula is that it splits the multivariate distribution into its margins and a pure dependency component. In other words, it captures the dependency between variables, eliminating the impact of the marginal distributions as introduced in the previous subsection.

Furthermore, we incorporate this procedure within an HMM framework. We denote the underlying Markov variable X_t as a dependency type variable. If $x_t = i$, the parameters $(\boldsymbol{\theta}^{(i)}, s^{(i)})$ determined by state $i = 1, \ldots, M$ take values on $\Theta \times S$, where S is a set of discrete candidate states corresponding to different dependency structures of the HAC, and Θ is a compact subset of $\mathbb{R}^{d-1}$ in which the HAC parameters take their values. Therefore,

$$f_i(\cdot) = c\left\{F_1^{\mathfrak{m}}(y_1), F_2^{\mathfrak{m}}(y_2), \ldots, F_d^{\mathfrak{m}}(y_d), \boldsymbol{\theta}^{(i)}, s^{(i)}\right\} f_1^{\mathfrak{m}}(y_1) f_2^{\mathfrak{m}}(y_2) \cdots f_d^{\mathfrak{m}}(y_d), \tag{8}$$

with $f_i^{\mathfrak{m}}(y_i)$ being the marginal densities, $F_i^{\mathfrak{m}}(y_i)$ the marginal cdf and $c(\cdot)$ the copula density, which is defined in assumption A.4 in Section 3.

Let $\boldsymbol{\theta}^{(i)} = (\theta_{i1}, \ldots, \theta_{i,d-1})^\top$ be the dependency parameters of the copulae starting from the lowest up to the highest level connected with a fixed state $x_t = i$ and corresponding density $f_i(.)$. Refining the algorithm of Okhrin et al. (2013), the multistage maximum likelihood estimator $(\hat{\boldsymbol{\theta}}^{(i)}, \hat{s}^{(i)})$ solves the system

$$\left(\frac{\partial \mathcal{L}_1}{\partial \theta_{i1}}, \ldots, \frac{\partial \mathcal{L}_{d-1}}{\partial \theta_{id-1}}\right)^\top = \mathbf{0}, \tag{9}$$

where

$$\mathcal{L}_j = \sum_{t=1}^{T} w_{it} l_{ij}(Y_t), \quad \text{for } j = 1, \ldots, d-1,$$

$$l_{ij}(Y_t) = \log\left(c\left[\{\hat{F}_m^{\mathfrak{m}}(y_{tm})\}_{m\in\{1,\ldots,j\}}; \{\theta_{i\ell}\}_{\ell=1,\ldots,j-1}, s_m^{(i)}\right] \prod_{m\in\{1,\ldots,j\}} \hat{f}_m^{\mathfrak{m}}(y_{tm})\right)$$

$$\text{for } t = 1, \ldots, T.$$

where j denotes the layers of the tree structure, and $\hat{F}_m^{\mathfrak{m}}(\cdot)$ is an estimator (either nonparametric with $\hat{F}_m^{\mathfrak{m}}(x) = (T+1)^{-1} \sum_{t=1}^{T} \mathbf{1}(Y_{tm} \le x)$ or parametric $\hat{F}_m^{\mathfrak{m}}(x) = F_m^{\mathfrak{m}}(x, \hat{\boldsymbol{\alpha}}_m)$) of the marginal cdf $F_m^{\mathfrak{m}}(\cdot)$, where $\hat{\boldsymbol{\alpha}}_m$ stand for estimated parameters of a marginal distribution. Note that a nonparametric estimation of the margins would lead to our estimation's having a semiparametric nature. The marginal densities $\hat{f}_m^{\mathfrak{m}}(\cdot)$ are estimated parametrically or nonparametrically (kernel density estimation) corresponding to the estimation of the marginal distribution functions, and w_{it} is the weight associated with state i and time t, see (14). Chen and Fan (2006) and Okhrin et al. (2013) provide the asymptotic behavior of the estimates.

https://doi.org/10.1017/S0266466614000607 Published online by Cambridge University Press

2.3. Likelihood estimation

For the estimation of the HMM HAC model, we adopt the EM algorithm, see Dempster, Laird, and Rubin (1977), also known as the Baum–Welch algorithm in the context of HMM. Recall the full likelihood $p_T(y_{0:T}; x_{0:T})$ in (6) and the partial likelihood $p_T(y_{0:T})$ in (7), and the log likelihood:

$$\log\{p_T(y_{0:T})\} = \log\left\{\sum_{x_0=1}^{M}\cdots\sum_{x_n=1}^{M}\pi_{x_0} f_{x_0}(y_0;\boldsymbol{\theta}^{(x_0)})\prod_{t=1}^{T} p_{x_{t-1}x_t} f_{x_t}(y_t;\boldsymbol{\theta}^{(x_t)}, s^{(x_t)})\right\}. \tag{10}$$

The EM algorithm suggests estimating a sequence of parameters $\mathfrak{g}_{(r)} \stackrel{\text{def}}{=} (P_{(r)}, \boldsymbol{\theta}_{(r)}, \mathbf{s}_{(r)})$ (for the rth iteration) by iterative maximization of $\mathcal{Q}(\mathfrak{g}; \mathfrak{g}_{(r)})$ with

$$\mathcal{Q}(\mathfrak{g}; \mathfrak{g}_{(r)}) \stackrel{\text{def}}{=} \mathsf{E}_{\mathfrak{g}_{(r)}}\{\log p_T(Y_{0:T}; X_{0:T})|Y_{0:T} = y_{0:T}\}.$$

That is, one carries out the following two steps:

- (a) E-step: compute $\mathcal{Q}(\mathfrak{g}; \mathfrak{g}_{(r)})$,
- (b) M-step: choose the update parameters $\mathfrak{g}_{(r+1)} = \arg\max_{\mathfrak{g}} \mathcal{Q}(\mathfrak{g}; \mathfrak{g}_{(r)})$.

The essence of the EM algorithm is that $\mathcal{Q}(\mathfrak{g}; \mathfrak{g}_{(r)})$ can be used as a substitute for $\log p_T(y_{0:T}; x_{0:T}; \theta)$, see Cappé, Moulines, and Rydén (2005).

In our setting, we may write $\mathcal{Q}(\mathfrak{g}; \mathfrak{g}_{(r)})$ as:

$$\begin{aligned}\mathcal{Q}(\mathfrak{g}; \mathfrak{g}_{(r)}) &= \sum_{i=1}^{M}\mathsf{E}_{\mathfrak{g}_{(r)}}[\mathbf{1}\{X_0 = i\}\log\{\pi_i f_i(y_0)\}|Y_{0:T} = y_{0:T}] \qquad (11)\\ &\quad + \sum_{t=1}^{T}\sum_{i=1}^{M}\mathsf{E}_{\mathfrak{g}_{(r)}}[\mathbf{1}\{X_t = i\}\log f_i(y_t)|Y_{0:T} = y_{0:T}]\\ &\quad + \sum_{t=1}^{T}\sum_{i=1}^{M}\sum_{j=1}^{M}\mathsf{E}_{\mathfrak{g}_{(r)}}[\mathbf{1}\{X_t = j\}\mathbf{1}\{X_{t-1} = i\}\log\{p_{ij}\}|Y_{0:T} = y_{0:T}]\\ &= \sum_{i=1}^{M}\mathrm{P}_{\mathfrak{g}_{(r)}}(X_0 = i|Y_{0:T} = y_{0:T})\log\{\pi_i f_i(y_0)\}\\ &\quad + \sum_{t=1}^{T}\sum_{i=1}^{M}\mathrm{P}_{\mathfrak{g}_{(r)}}(X_t = i|Y_{0:T} = y_{0:T})\log f_i(y_t)\\ &\quad + \sum_{t=1}^{T}\sum_{i=1}^{M}\sum_{j=1}^{M}\mathrm{P}_{\mathfrak{g}_{(r)}}(X_{t-1} = i, X_t = j|Y_{0:T} = y_{0:T})\log\{p_{ij}\}, \qquad (12)\end{aligned}$$

where $f_i(\cdot)$ is as in (8). The E-step, in which $\mathrm{P}_{\mathfrak{g}_{(r)}}(X_t = i|Y_{0:T}), \mathrm{P}_{\mathfrak{g}_{(r)}}(X_{t-1} = i, X_t = j|Y_{0:T})$ are evaluated, is carried out by the forward–backward algorithm

https://doi.org/10.1017/S0266466614000607 Published online by Cambridge University Press

and the M-step is explicit in the p_{ij}s and the π_is. Adding constraints to (12) yields

$$\mathfrak{L}(\mathfrak{g}, \lambda; \mathfrak{g}') = \mathcal{Q}(\mathfrak{g}; \mathfrak{g}') + \sum_{i=1}^{M} \lambda_i \left(1 - \sum_{j=1}^{M} p_{ij}\right). \tag{13}$$

For the M-step, we need to take the first order partial derivatives, and plug into (13). So the dependency parameters $\boldsymbol{\theta}$ and the structure parameters $\mathbf{s}$ need to be estimated iteratively, for $\boldsymbol{\theta}^{(i)}$ ($\boldsymbol{\theta}^{(i)} = \{\theta_{i1}, \ldots, \theta_{i(d-1)}\}$):

$$\frac{\partial \mathfrak{L}(\mathfrak{g}, \lambda; \mathfrak{g}')}{\partial \theta_{ij}} = \sum_{t=1}^{T} \mathrm{P}_{\mathfrak{g}'}(X_t = i | Y_{0:T}) \partial \log f_i(y_t) / \partial \theta_{ij}. \tag{14}$$

To simplify the procedure, we adopt the HAC estimation method (9) with weights $w_{it} \stackrel{\text{def}}{=} \mathrm{P}_{\mathfrak{g}'}(X_t = i | Y_{0:T})$. We also fix $\pi_i, i = 1, \ldots, M$, as this influences only the first observation x_0 which may be considered also as given and fixed. Maximizing (12) w.r.t. π_i would return the first derivative with one observation y_0. Also as the previous information for the distribution of x_0 is not available, our EM algorithm would not involve updating π_i. The estimation of the transition probabilities p_{ij} follows:

$$\frac{\partial \mathfrak{L}(\mathfrak{g}, \lambda; \mathfrak{g}')}{\partial p_{ij}} = \sum_{t=1}^{T} \frac{\mathrm{P}_{\mathfrak{g}'}(X_{t-1} = i, X_t = j | Y_{0:T})}{p_{ij}} - \lambda_i, \tag{15}$$

$$\frac{\partial \mathfrak{L}(\mathfrak{g}, \lambda; \mathfrak{g}')}{\partial \lambda_i} = 1 - \sum_{j=1}^{M} p_{ij}. \tag{16}$$

Equating (15) and (16) yields

$$\hat{p}_{ij} = \frac{\sum_{t=1}^{T} \mathrm{P}_{\mathfrak{g}'}(X_{t-1} = i, X_t = j | Y_{0:T})}{\sum_{t=1}^{T} \sum_{l=1}^{M} \mathrm{P}_{\mathfrak{g}'}(X_{t-1} = i, X_t = l | Y_{0:T})}. \tag{17}$$

3. THEORETICAL RESULTS

In this section, we discuss the conditions needed to derive the consistency and the asymptotic properties of our estimates. We then state our main theoretical theorems. Throughout the theory we concentrate on the most interesting case: a semi-parametric estimation with nonparametric margins.

Assumptions.

A.1 $\{X_t\}$ is a stationary, strictly irreducible, and aperiodic Markov process of order one with final discrete state, and $\{Y_t\}_{t=1}^{T}$ are conditionally independent given $\{X_t\}_{t=1}^{T}$ and generated from an HAC HMM model with parameters $\{s^{*(i)}, \theta^{*(i)}, \pi^*, \{p^*_{ij}\}_{i,j}\}, i, j = 1, \ldots, d$.

https://doi.org/10.1017/S0266466614000607 Published online by Cambridge University Press

It is worth noting that A.1 is the basic assumption on the evolution of a hidden Markov chain. One key property is that given one realization of the path of $\{X_t\}$, the conditional distributions of $\{Y_t\}_{t=1}^{T}$ are totally fixed. But $\{Y_t\}$ will be dependent and will even have a finite mixture distribution from the given parametric family. The evolution of $\{X_t\}$ will later be linked to the dependency parameters of the state space distribution of $\{Y_t\}$.

A.2 The family of mixtures of at most M elements $\{f(y;\boldsymbol{\theta}^{(i)}, s^{(i)}) : \boldsymbol{\theta}^{(i)} \in \Theta^{(i)}, s^{(i)} \in S\}$ is identifiable w.r.t. the parameters and structures:

$$\sum_{i=1}^{M} \alpha_i f\left(y;\boldsymbol{\theta}^{(i)}, s^{(i)}\right) = \sum_{i=1}^{M} \alpha_i' f\left(y;\boldsymbol{\theta}'^{(i)}, s'^{(i)}\right) \quad a.e. \tag{18}$$

$$then, \sum_{i=1}^{M} \alpha_j \delta_{\boldsymbol{\theta}^{(i)}, s^{(i)}} = \sum_{i=1}^{M} \alpha_i' \delta_{\boldsymbol{\theta}'^{(i)}, s'^{(i)}}, \tag{19}$$

defining $\delta_{\boldsymbol{\theta}^{(i)}, s^{(i)}}$ as the distribution function for a point mass in Θ associated with the structure $s^{(i)}$, noting that $\boldsymbol{\theta}^{(i)} = \boldsymbol{\theta}'^{(i)}$ is only meaningful when $s^{(i)} = s'^{(i)}$.

The property of identifiability is nothing else than the construction of a finite mixture model, see McLachlan and Peel (2000). As a copula is a special form of a multivariate distribution, similar techniques may be applied to get identifiability also in the case of copulae. The family of copula mixtures has been thoroughly investigated in Caia, Chen, Fan, and Wang (2006) while developing estimation techniques. In that general case, one should be careful, as the general copula class is very wide and its mixture identification may cause some problems because of the different forms of the densities. The very construction of the HAC narrows this class. Imposing the same generator functions on all levels of the HAC, we restrict the family to the vector of parameters and the tree structure, see also Okhrin et al. (2013). Moreover, we restrict the classes to only binary trees with distinct parameters to avoid identifiability issues induced by the case of the same parameter values on each layer of a tree. Our preliminary numerical analysis shows that the HAC fulfills the identifiability property for all the structures and parameters used in this study.

A.3 The true marginal distribution $f_m^{\mathrm{m}}(\cdot) \in \mathbf{C}^2$, and the derivatives up to a second order are bounded for all $m = 1, \ldots, d$. Also $\sqrt{f^{\mathrm{m}}}$ is absolute continuous. In the case of a nonparametric estimation for $f_i^{\mathrm{m}}(\cdot) \in \mathbf{C}^2$, one needs also to ensure that the kernel function $K(\cdot) \in C^2$ subject to $\int_B K(u)du = 1$, has support on a compact set B, is symmetric, and has integrable first derivative.

We would like to focus on the dependency parameter, therefore in the following setting, we simply assume that the marginal processes $y_{t1}, y_{t2}, \ldots, y_{td}$ are identically distributed.

A.4 $\mathsf{E}\{|\log f_i(y)|\} < \infty$, for $i = 1, \ldots, M$, $\forall s^{(i)} \in S$. Define the copulae density function $c(u_1, u_2, \ldots, u_d, \boldsymbol{\theta}^{(i)}, s^{(i)}) \stackrel{\text{def}}{=} \partial^d C(u_1, u_2, \ldots, u_d, , \boldsymbol{\theta}^{(i)}, s^{(i)}) / \partial u_1 \partial u_2 \cdots \partial u_d$, then $\log c(u_1, u_2, \ldots, u_d, \boldsymbol{\theta}^{(i)}, s^{(i)})$ as well as its first and second

https://doi.org/10.1017/S0266466614000607 Published online by Cambridge University Press

partial derivatives w.r.t. u_is and $\boldsymbol{\theta}^{(i)}$ are well defined for $((0,1)^d \times \Theta^{(i)})$. Also, their suprema in a compact set $((E^d) \times \Theta^{(i)})$ $(E^d \in [0,1]^d)$ has finite moments up to the order four.

A.5 For every $\boldsymbol{\theta}^{(i)} \in \Theta$, and any particular structure $s \in S$,

$$\mathsf{E}\left[\sup_{\|\boldsymbol{\theta}'^{(i)}-\theta^{(i)}\|<\delta}\{f_i(Y_1,\theta'^{(i)},s)\}^+\right] < \infty,$$

for some $\delta > 0$.

A.6 The true point $\boldsymbol{\theta}^*$ is an interior point of Θ.

A.7 There exists a constant δ^0, such that $\mathrm{P}(\sup_{\|\boldsymbol{\theta}'^{(i)}-\boldsymbol{\theta}^{(i)}\|<\delta^0} \max_{i,j} \mathsf{E}\frac{\{f_i(Y_1,\boldsymbol{\theta}',s)\}}{\{f_j(Y_1,\boldsymbol{\theta}',s)\}} = \infty | X_1 = i) < 1$.

Denote by $p_T(y_{0:T};\upsilon,\omega)$ the density in (7) with parameters $\{\upsilon,\omega\} \in \{V,\Omega\}$ as described in the Appendix 7.2. Define $\hat{\boldsymbol{\theta}}^{(i)}, \hat{s}^{(i)}$ as $\hat{\boldsymbol{\theta}}^{(i)}(\hat{\upsilon},\hat{\omega})$, and $\hat{s}^{(i)}(\hat{\upsilon},\hat{\omega})$ with $(\hat{\upsilon},\hat{\omega})$ being the point where $p_T(y_{0:T};\upsilon,\omega)$ achieves its maximum value over the parameter space $\{V,\Omega\}$.

It is known that HMM is not itself identifiable, as a permutation of states would yield the same value for $p_T(y_{0:T};\upsilon,\omega)$. We assume therefore $\boldsymbol{\theta}^{*(j)}$s and $s^{*(j)}$s to be distinct in the sense that for any $s^{*(i)} = s^{*(j)}, i \neq j$ we have $\boldsymbol{\theta}^{*(i)} \neq \boldsymbol{\theta}^{*(j)}$.

THEOREM 3.1. *Under A.1–A.7, we find the corresponding structure:*

$$\lim_{T\to\infty} \min_{i\in 1,\ldots,M} \mathrm{P}(\hat{s}^{(i)} = s^{*(i)}) = 1. \tag{20}$$

Moreover,

THEOREM 3.2. *Assume that A.1–A.7 hold then the parameter* $\hat{\boldsymbol{\theta}}^{(i)}$ *satisfies,* $\forall \varepsilon > 0$*:*

$$\lim_{T\to\infty} \max_{i\in 1,\ldots,M} \mathrm{P}\left(|\hat{\boldsymbol{\theta}}^{(i)} - \boldsymbol{\theta}^{*(i)}| > \varepsilon | \hat{s}^{(i)} = s^{*(i)}\right) = 0. \tag{21}$$

In addition, we can also establish asymptotic normality results for parameters.

THEOREM 3.3. *Assume that A.1–A.7 hold , and given that* $s^{*(i)}$ *is correctly estimated, which is an event with probability tending to* 1*, we have*

$$\sqrt{T}\left\{\hat{\boldsymbol{\theta}} - \boldsymbol{\theta}\right\} \to \mathsf{N}(0,\Sigma^*), \tag{22}$$

where Σ^* *is the asymptotic covariance function, defined as* $\Sigma^* \stackrel{\text{def}}{=} B^{-1}\,\mathsf{Var}(\sqrt{T}A)\,B^{-1}$*, where* B, A *are defined in the Appendix in (A.19).*

The proofs are presented in the Appendix.

4. SIMULATION

The estimation performance of HMM HAC is evaluated in this section: subsection I aims to investigate whether the performance of the estimation is affected

https://doi.org/10.1017/S0266466614000607 Published online by Cambridge University Press

by 1) adopting a nonparametric or parametric margins; 2) introducing a GARCH dependency in the marginal time series. Subsection II presents results for a five-dimensional time series model. In subsection III we compare the DCC method and our HMM HAC method. All the simulations show that our algorithm converges after a few iterations with moderate estimation errors, and the results are robust with respect to different estimation methods for the margins. Moreover our method dominates the DCC one.

Regarding the selection of the orders, in both the simulations and the applications, we have started with a model with three states, which is suggested by the initial moving window analysis described later. In the applications, the number of states will even be degenerated to two or one for some windows. This suggests that three states are sufficient for model estimations. However, one can consider general BIC or AIC criteria for selecting the number of states.

4.1. Simulation I

In this subsection, a three-dimensional generating process has fixed marginal distributions: $Y_{t1}, Y_{t2}, Y_{t3} \sim \mathsf{N}(0,1)$. To study the effect of deGARCH step in our application (DeGARCH is meant by prefitting marginal time series with a GARCH model, and take the residuals for estimation in later steps.), we simulated also according to a GARCH(1,1) model,

$$Y_{tj} = \mu_{tj} + \sigma_{tj}\varepsilon_{tj} \text{ with } \sigma_{tj}^2 = \omega_j + \alpha_j \sigma_{t-1j}^2 + \beta_j (Y_{t-1j} - \mu_{t-1j})^2, \tag{23}$$

with parameters $\omega_j = 10^{-6}, \alpha_j = 0.8, \beta_j = 0.1$, with standard normal residuals $\varepsilon_{t1}, \varepsilon_{t2}, \varepsilon_{t3} \sim \mathsf{N}(0,1)$. The dependence structure is modeled through HAC with Gumbel generators. Let us consider now a Monte Carlo setup where the setting employs realistic models. The three states with $M = 3$ are as follows:

$$C\left\{u_1, C(u_2, u_3; \theta_1^{(1)} = 1.3); \theta_2^{(1)} = 1.05\right\} \quad \text{for } i = 1,$$
$$C\left\{u_2, C(u_3, u_1; \theta_1^{(2)} = 2.0); \theta_2^{(2)} = 1.35\right\} \quad \text{for } i = 2,$$
$$C\left\{u_3, C(u_1, u_2; \theta_1^{(3)} = 4.5); \theta_2^{(3)} = 2.85\right\} \quad \text{for } i = 3,$$

where the dependency parameters correspond to Kendall's τs ranging between 0.05 and 0.78, which is typical for financial data. The transition matrix is chosen as:

$$P = \begin{pmatrix} 0.982 & 0.010 & 0.008 \\ 0.008 & 0.984 & 0.008 \\ 0.003 & 0.002 & 0.995 \end{pmatrix},$$

with initial probabilities as $\pi = (0.2, 0.1, 0.7)$ and sample size $T = 2000$. Figure 3 presents the underlying states and a marginal plot of the generated three-dimensional time series. No state switching patterns are evident from the marginal plots. Figure 4, however, clearly displays the switching of dependency

https://doi.org/10.1017/S0266466614000607 Published online by Cambridge University Press

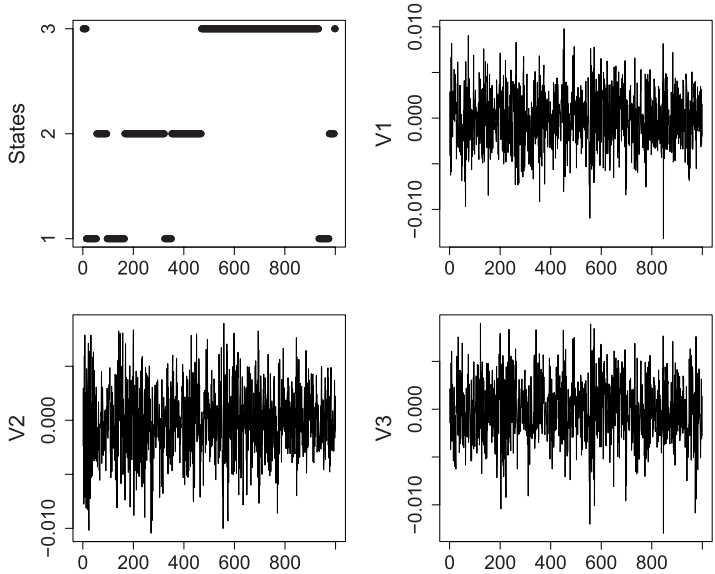

FIGURE 3. The underlying sequence x_t (upper left panel), marginal plots of $(y_{t1}, y_{t2}, y_{t3})(t = 0, \ldots, 1000)$.

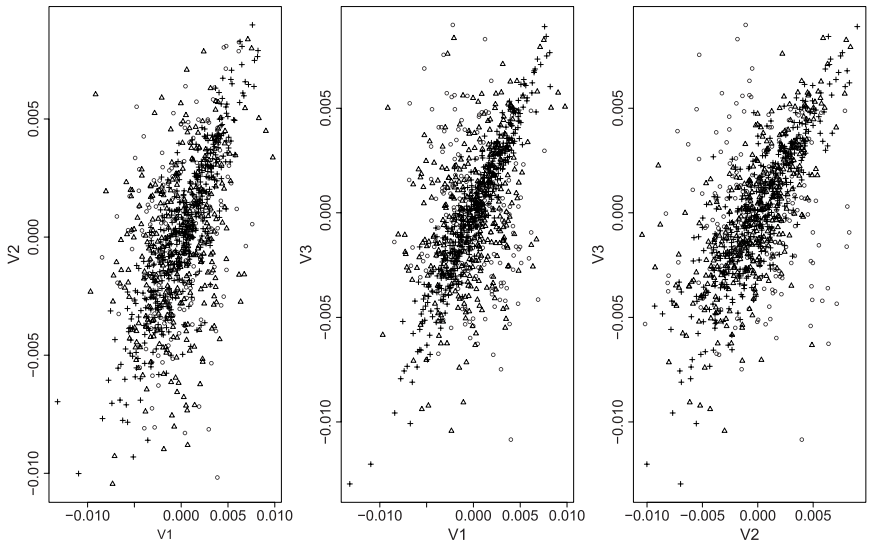

FIGURE 4. Snapshots of pairwise scatter plots of dependency structures $(t = 0, \ldots, 1000)$, the (y_{t1}) vs. (y_{t2}) (left), the (y_{t1}) vs. (y_{t3}) (middle), and the (y_{t2}) vs. (y_{t3})(right).

https://doi.org/10.1017/S0266466614000607 Published online by Cambridge University Press

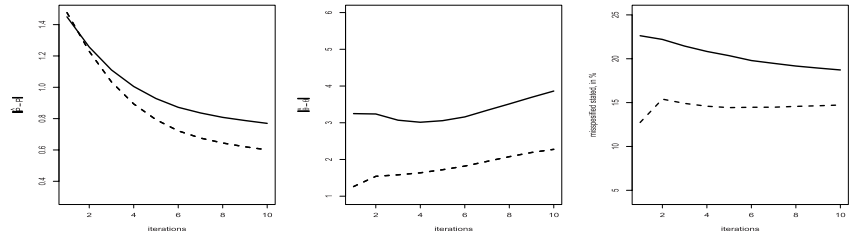

(a) With GARCH effects in the margins, nonparametrically estimated margins

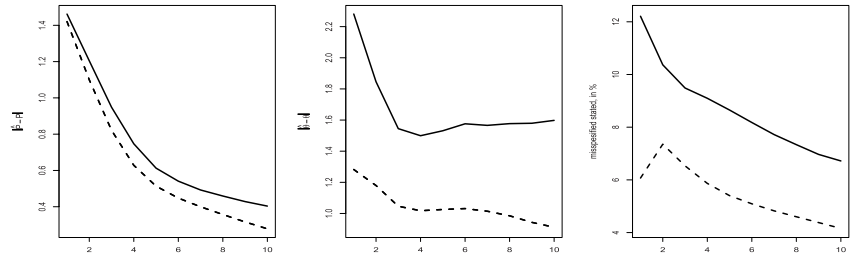

(b) Without GARCH effects in the margins, nonparametrically estimated margins

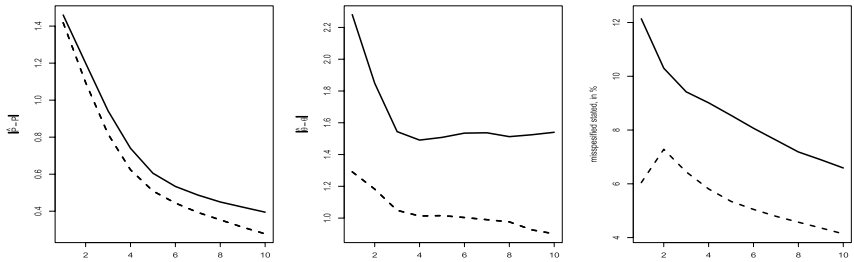

(c) Without GARCH effects in the margins, parametric margins

FIGURE 5. The averaged estimation errors for the transition matrix (left panel), parameters (middle panel), and convergence of states (right panel). Estimation starts from near true value (dashed); starts from values obtained by rolling window (solid). x-axis represents iterations. Number of repetitions is 1000.

patterns. The circles, triangles, and crosses correspond to the observations from states $i = 1, 2, 3$, respectively.

Generally, the iteration procedure stops after around ten steps. Figure 5 presents the deviations from their true values of the estimated states, the transition matrix, and the parameters for the first ten iterations of one sample. Since the starting values may influence the results, a moving window estimation is proposed to decide the initial parameters. The dashed black and solid black lines show, respectively, how the estimators behave with the initial values close to the true (dashed) and initial values obtained from the proposed rolling window algorithm

https://doi.org/10.1017/S0266466614000607 Published online by Cambridge University Press

(solid). By "close to the true initial states", we mean true structures with parameters all shifted up by 0.5 from the true ones. For "rolling window algorithm" we estimate HAC for overlapping windows of width 100, and then take the M most frequent structures with averaged parameters as initial states. The left panel of Figure 5 shows the (L_1) difference $(\sum_{i,j=1}^{d} |\hat{p}_{ij} - p_{ij}|)$ of the true transition matrix from the estimated ones at each iteration, we see that for the three particular samples, the values all converge to around 0.4, which are moderately small; the middle panel is the sum of the estimated parameter errors of the four states with the correctly estimated states, we see that the accumulated errors are different depending on the different starting values; the right panel presents the percentage of wrongly estimated states, in all cases the percentage of wrongly estimated states is smaller than 8%. One can see that our choice of initial values can perform as well as the true ones through showing small differences, and our results from more iterations further confirm this.

Generally, the iteration procedure stops after around ten steps. Figure 5 presents the deviations from their true values of the estimated states, the transition matrix, and the parameters for the first ten iterations of one sample. Since the starting values may influence the results, a moving window estimation is proposed to decide the initial parameters. The dashed black and solid black lines show, respectively, how the estimators behave with the initial values close to the true (dashed) and initial values obtained from the proposed rolling window algorithm (solid). By "close to the true initial states", we mean true structures with parameters all shifted up by 0.5 from the true ones. For "rolling window algorithm" we estimate HAC for overlapping windows of width 100, and then take the M most frequent structures with averaged parameters as initial states. The left panel of Figure 5 shows the (L_1) difference $(\sum_{i,j=1}^{d} |\hat{p}_{ij} - p_{ij}|)$ of the true transition matrix from the estimated ones at each iteration, we see that for the three particular samples, the values all converge to around 0.4, which are moderately small; the middle panel is the sum of the estimated parameter errors of the four states with the correctly estimated states, we see that the accumulated errors are different depending on the different starting values; the right panel presents the percentage of wrongly estimated states, in all cases the percentage of wrongly estimated states is smaller than 8%. One can see that our choice of initial values can perform as well as the true ones through showing small differences, and our results from more iterations further confirm this.

Finally, we summarize our estimation results over 1000 repetitions. In Tables 1–2, we report the averaged estimation values with standard deviations (in brackets) and MSE (in brackets) for the estimated states, the transition matrix, and the parameters. Table 1 presents the results with the marginal time series being generated as just identically distributed data, while Table 2 presents the results with the marginal DGPs being GARCH(1,1). For the impact of estimating the copula model on estimated standardized residuals (after GARCH fitting, for example), we have also included a comparison of the estimation on the deGARCHed residuals (nonparametrically estimated margins).

https://doi.org/10.1017/S0266466614000607 Published online by Cambridge University Press

TABLE 1. Simulation results for the marginal time series being generated as identically distributed data, sample size $T = 2000$, 1000 repetitions, standard deviations and MSEs are provided in brackets

			True	Rol. Win.	True Str.
Nonparametric Margins	C_1	$\theta_1^{(1)}$	1.05	1.030 (0.046, 0.003)	1.057 (0.068, 0.005)
		$\theta_2^{(1)}$	1.30	1.313 (0.156, 0.025)	1.308 (0.083, 0.007)
	C_2	$\theta_1^{(2)}$	1.35	1.366 (0.121, 0.015)	1.346 (0.182, 0.033)
		$\theta_2^{(2)}$	2.00	2.556 (1.052, 1.416)	3.212 (1.991, 5.433)
	C_3	$\theta_1^{(3)}$	2.85	2.854 (0.073, 0.005)	2.854 (0.073, 0.005)
		$\theta_2^{(3)}$	4.50	4.497 (0.133, 0.018)	4.496 (0.130, 0.017)
	rat. of correct states			0.958 (0.029)	0.933 (0.056)
	$\sum_{i,j=1}^{d} \lvert\hat{p}_{ij} - p_{ij}\rvert$			0.278 (0.230)	0.404 (0.307)
	rat. of correct structures			0.949	0.918
Parametric Margins	C_1	$\theta_1^{(1)}$	1.05	1.030 (0.041, 0.002)	1.056 (0.066, 0.004)
		$\theta_2^{(1)}$	1.30	1.310 (0.154, 0.024)	1.306 (0.087, 0.008)
	C_2	$\theta_1^{(2)}$	1.35	1.365 (0.130, 0.017)	1.344 (0.173, 0.030)
		$\theta_2^{(2)}$	2.00	2.544 (0.962, 1.221)	3.157 (1.906, 4.971)
	C_3	$\theta_1^{(3)}$	2.85	2.855 (0.074, 0.006)	2.854 (0.074, 0.005)
		$\theta_2^{(3)}$	4.50	4.513 (0.133, 0.018)	4.513 (0.132, 0.018)
	rat. of correct states			0.959 (0.029)	0.934 (0.056)
	$\sum_{i,j=1}^{d} \lvert\hat{p}_{ij} - p_{ij}\rvert$			0.278 (0.232)	0.395 (0.297)
	rat. of correct structures			0.955	0.921
deGARCHing	C_1	$\theta_1^{(1)}$	1.05	1.030 (0.045, 0.002)	1.056 (0.067, 0.005)
		$\theta_2^{(1)}$	1.30	1.320 (0.264, 0.070)	1.307 (0.081, 0.007)
	C_2	$\theta_1^{(2)}$	1.35	1.367 (0.123, 0.015)	1.345 (0.166, 0.028)
		$\theta_2^{(2)}$	2.00	2.577 (1.273, 1.953)	3.180 (1.976, 5.297)
	C_3	$\theta_1^{(3)}$	2.85	2.852 (0.074, 0.005)	2.852 (0.074, 0.005)
		$\theta_2^{(3)}$	4.50	4.489 (0.133, 0.018)	4.488 (0.130, 0.017)
	rat. of correct states			0.958 (0.029)	0.933 (0.056)
	$\sum_{i,j=1}^{d} \lvert\hat{p}_{ij} - p_{ij}\rvert$			0.280 (0.234)	0.399 (0.299)
	rat. of correct structures			0.950	0.919

Also the estimation for different ways of deciding starting values are shown: "close to the true initial states" (True str), rolling window algorithm (Rol. Win.). Apparently, nonparametric or parametric estimation of the margins does not make big differences; this is also true for the prewhitening step. Regarding the precision

https://doi.org/10.1017/S0266466614000607 Published online by Cambridge University Press

TABLE 2. Simulation results for the marginal DGPs (data generating processes) being GARCH(1,1), sample size $T = 2000$, 1000 repetitions, standard deviations and MSEs are provided in brackets

			True	Rol. Win.	True Str.
Nonparametric Margins	C_1	$\theta_1^{(1)}$	1.05	1.100 (0.888, 0.791)	1.138 (0.080, 0.014)
		$\theta_2^{(1)}$	1.30	1.407 (0.888, 0.800)	1.246 (0.080, 0.009)
	C_2	$\theta_1^{(2)}$	1.35	1.403 (1.473, 2.173)	1.436 (2.608, 6.089)
		$\theta_2^{(2)}$	2.00	3.288 (1.473, 3.829)	5.106 (2.608, 16.449)
	C_3	$\theta_1^{(3)}$	2.85	2.772 (0.936, 0.882)	2.790 (0.941, 0.889)
		$\theta_2^{(3)}$	4.50	4.570 (0.936, 0.881)	4.606 (0.941, 0.897)
	rat. of correct states			0.853 (0.054)	0.813 (0.061)
	$\sum_{i,j=1}^{d} \lvert\hat{p}_{ij} - p_{ij}\rvert$			0.601 (0.217)	0.770 (0.242)
	rat. of correct structures			0.853	0.757
Parametric Margins	C_1	$\theta_1^{(1)}$	1.05	1.205 (1.261, 1.614)	1.107 (0.079, 0.009)
		$\theta_2^{(1)}$	1.30	1.843 (1.261, 1.885)	1.145 (0.079, 0.030)
	C_2	$\theta_1^{(2)}$	1.35	1.577 (1.381, 1.959)	1.838(1.612, 2.837)
		$\theta_2^{(2)}$	2.00	3.150 (1.381, 3.230)	3.480 (2.270, 7.343)
	C_3	$\theta_1^{(3)}$	2.85	3.879 (1.453, 3.170)	3.906 (1.523, 3.435)
		$\theta_2^{(3)}$	4.50	6.390 (1.453, 5.683)	6.592 (1.523, 6.696)
	rat. of correct states			0.732 (0.080)	0.747 (0.053)
	$\sum_{i,j=1}^{d} \lvert\hat{p}_{ij} - p_{ij}\rvert$			0.761 (0.179)	0.760 (0.156)
	rat. of correct structures			0.358	0.323
deGARCHing	C_1	$\theta_1^{(1)}$	1.05	1.030 (0.736, 0.542)	1.067 (0.141, 0.020)
		$\theta_2^{(1)}$	1.30	1.333 (0.736, 0.543)	1.305 (0.141, 0.020)
	C_2	$\theta_1^{(2)}$	1.35	1.356 (1.059, 1.122)	1.333 (1.755, 3.080)
		$\theta_2^{(2)}$	2.00	2.579 (1.059, 1.457)	3.351 (1.755, 4.905)
	C_3	$\theta_1^{(3)}$	2.85	2.835 (0.816, 0.666)	2.833 (0.816, 0.666)
		$\theta_2^{(3)}$	4.50	4.452 (0.816, 0.668)	4.451 (0.816, 0.668)
	rat. of correct states			0.958 (0.028)	0.925 (0.058)
	$\sum_{i,j=1}^{d} \lvert\hat{p}_{ij} - p_{ij}\rvert$			0.299 (0.235)	0.460 (0.325)
	rat. of correct structures			0.938	0.916

of the estimation, one sees that when the true GDP is GARCH(1,1), the prewhitening step is necessary to guarantee the quality of estimation. Also we see that for the parameter $\theta_2^{(2)}$ the estimation errors are larger. The standard deviations of the design matrix are also relatively high. This is due to our selected design matrix

https://doi.org/10.1017/S0266466614000607 Published online by Cambridge University Press

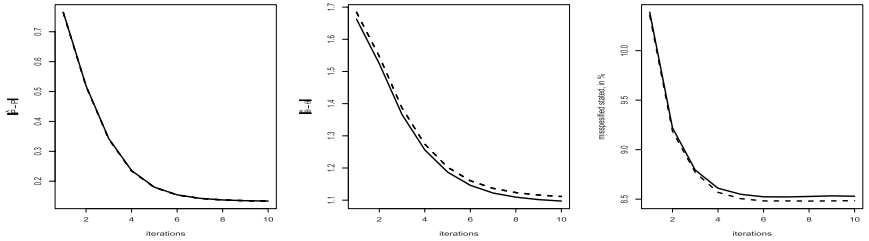

FIGURE 6. The averaged estimation errors for transition matrix (left panel), parameters (middle panel), convergence of states (right panel). Estimation starts from near true value (dashed); starts from values obtained by rolling window(solid). x-axis represents iterations. Number of repetitions is 1000.

having very small off-diagonal values, so for some realizations we have too few observations for state 2 to achieve accurate estimates. One sees in our simulation II nicer results with a different transition matrix.

4.2. Simulation II

In this subsection, we consider a five-dimensional model. The marginal distributions are taken as: $Y_{t1}, Y_{t2}, Y_{t3}, Y_{t4}, Y_{t5} \sim \mathsf{N}(0,1)$. The dependence structure is modeled through an HAC with Gumbel generators as well. We set also three states $(M = 3)$:

$$C\big(u_1, C[u_2, C\{u_3, C(u_5, u_4; \theta_1 = 3.15); \theta_2 = 2.45\}; \theta_3 = 1.75]; \theta_4 = 1.05\big) \quad \text{for } i = 1,$$

$$C\big(u_3, C[u_5, C\{u_2, C(u_1, u_4; \theta_1 = 3.15); \theta_2 = 2.45\}; \theta_3 = 1.75]; \theta_4 = 1.05\big) \quad \text{for } i = 2,$$

$$C\big(u_5, C[u_4, C\{u_3, C(u_1, u_2; \theta_1 = 3.15); \theta_2 = 2.45\}; \theta_3 = 1.75]; \theta_4 = 1.05\big) \quad \text{for } i = 3,$$

the transition matrix is chosen as:

$$P = \begin{pmatrix} 0.82 & 0.10 & 0.08 \\ 0.08 & 0.84 & 0.08 \\ 0.03 & 0.02 & 0.95 \end{pmatrix},$$

and the initial probabilities are $\pi = (0.2, 0.1, 0.7)$ and $T = 2000$. Figure 7 shows the pairwise scatterplots of the observations generated from the above mentioned model. Similarly, Figure 6 and Table 3 present the estimation accuracy for this model. Although the computation is more demanding when the dimension is higher, we still can achieve the same degree of accuracy as in the three-dimensional case.

https://doi.org/10.1017/S0266466614000607 Published online by Cambridge University Press

TABLE 3. The summary of estimation accuracy in five dimensional model, standard deviations and MSEs are provided in brackets. The case of deGARCHing is with nonparametrically estimated margins

		True	Param. Margins	deGARCHing
C_1	$\theta_1^{(1)}$	1.05	1.019 (0.020, 0.001)	1.019 (0.020, 0.001)
	$\theta_2^{(1)}$	1.75	1.739 (0.077, 0.006)	1.741 (0.078, 0.006)
	$\theta_3^{(1)}$	2.45	2.584 (0.126, 0.034)	2.583 (0.126, 0.034)
	$\theta_4^{(1)}$	3.15	3.328 (0.194, 0.069)	3.318 (0.194, 0.066)
C_2	$\theta_1^{(2)}$	1.05	1.017 (0.021, 0.002)	1.017 (0.021, 0.002)
	$\theta_2^{(2)}$	1.75	1.795 (0.084, 0.009)	1.797 (0.084, 0.009)
	$\theta_3^{(2)}$	2.45	2.499 (0.120, 0.017)	2.499 (0.122, 0.017)
	$\theta_4^{(2)}$	3.15	3.381 (0.216, 0.100)	3.369 (0.215, 0.094)
C_3	$\theta_1^{(3)}$	1.05	1.044 (0.017, 0.000)	1.045 (0.018, 0.000)
	$\theta_2^{(3)}$	1.75	1.745 (0.041, 0.002)	1.747 (0.041, 0.002)
	$\theta_3^{(3)}$	2.45	2.492 (0.065, 0.006)	2.492 (0.065, 0.006)
	$\theta_4^{(3)}$	3.15	3.189 (0.094, 0.010)	3.185 (0.095, 0.010)
rat. of correct states			0.915 (0.011)	0.915 (0.011)
$\sum_{i,j=1}^{d} \lvert\hat{p}_{ij} - p_{ij}\rvert$			0.133 (0.054)	0.133 (0.054)
rat. of correct structures			1	1

4.3. Simulation III

To compare the forecasting performances of the different models, we simulate data from different true models: HMM GARCH, HMM id, and DCC, from which we simulate three-dimensional time series with $T-1$ observations. Then we fit different models (HMM GARCH, HMM id, HAC GARCH, HAC id, and DCC) with the $T-1$ observations at hand, and compare the one-step ahead distribution forecasts for the true and the estimated models. More specifically, for the distribution forecast comparison, we calculate the sum $y_{T1}+y_{T2}+y_{T3}$ (which may be thought of as the returns of an equally weighted portfolio).

Simulation of 1000 observations $y_{T1}+y_{T2}+y_{T3}$ allows us to compare the forecast distribution between the true model and the estimated models. Furthermore, we calculate Kolmogorov–Smirnov (KS) test statistics to measure the difference between the forecast distribution of observations from the true and the estimated model. The comparison has been done with $T = 250, 500, 1000$ Table 4 reports the means and the standard deviations of the KS test statistics for different models w.r.t. to the true one. We see obvious advantages of our method over the DCC model in the sense that our HMM GARCH model

https://doi.org/10.1017/S0266466614000607 Published online by Cambridge University Press

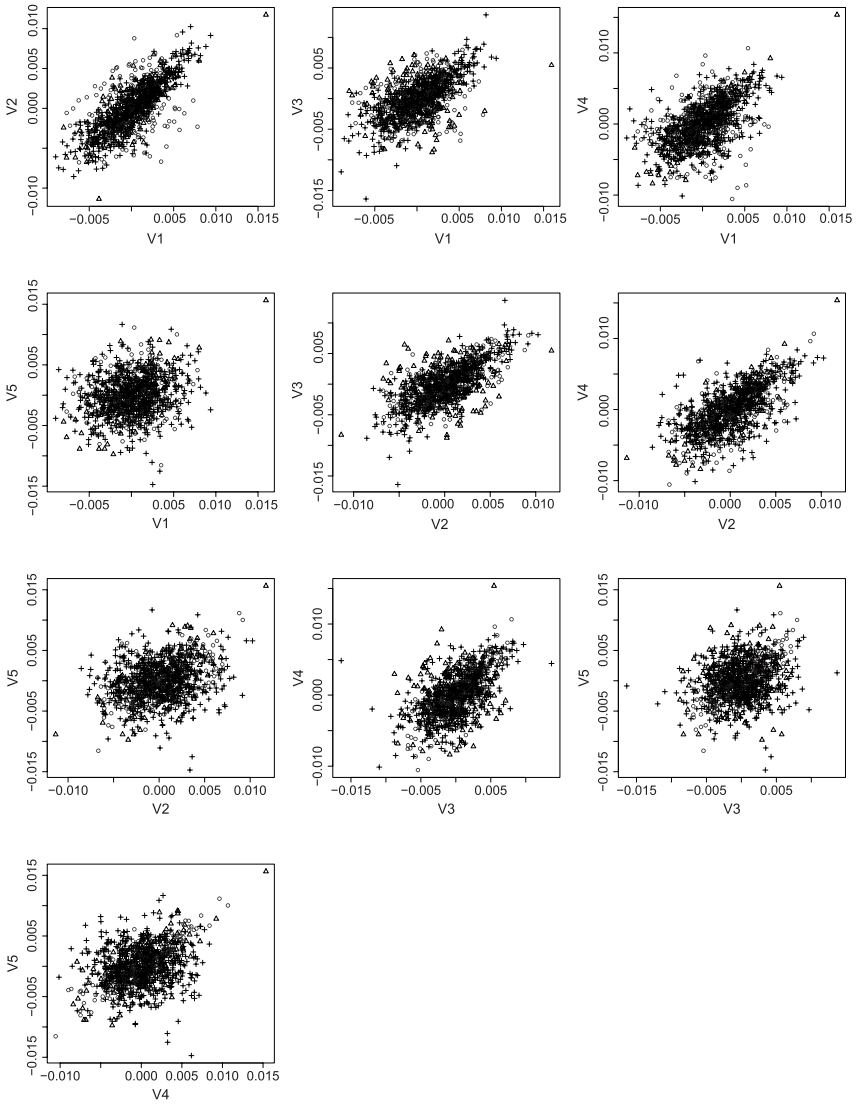

FIGURE 7. Snapshots of pairwise scatter plots of dependency structures ($t = 0, \ldots,$ 1000).

is in all cases closer on average to the forecast distribution of the true model than is the DCC model. Especially when the data generating processes are HMM GARCH or HMM ID. We use nonparametric estimated margins in this subsection.

https://doi.org/10.1017/S0266466614000607 Published online by Cambridge University Press

TABLE 4. The estimated mean KS test statistics (standard deviation) of the forecast distribution from the true model and the estimated model. Number of repetitions is 1000

True\Estimated	Sample size	HMMGARCH	HMM ID	DCC
HMM GARCH		**0.0899 (0.0353)**	0.1243 (0.0571)	0.1949 (0.1112)
DCC	250	**0.0607 (0.0241)**	0.0723 (0.0320)	0.0782 (0.0309)
HMM ID		0.0908 (0.0359)	**0.0867 (0.0345)**	0.1424 (0.0271)
HMMGARCH		**0.0889 (0.0338)**	0.1203 (0.0556)	0.2117 (0.0782)
DCC	500	**0.0541 (0.0194)**	0.0672 (0.0325)	0.0774 (0.0254)
HMM ID		**0.0936 (0.0331)**	0.0924 (0.0326)	0.1515 (0.0239)
HMM GARCH		**0.0869 (0.0321)**	0.1237 (0.0605)	0.3703 (0.1366)
DCC	1000	**0.0494 (0.0166)**	0.0659 (0.0320)	0.0823 (0.0392)
HMM ID		**0.0919 (0.0331)**	0.0907 (0.0322)	0.1509 (0.0213)

5. APPLICATIONS

To see how HMM HAC performs on a real data set, applications to financial and rainfall data are offered. A good model for the dynamics of exchange rates gives insights into exogenous economic conditions, such as the business cycle. It is also helpful for portfolio risk management and decisions on asset allocation. We demonstrate the performance of our proposed technique by applying it to forecasting the VaR of a portfolio and compare it with multivariate GARCH models (DCC, BEKK, etc.) The backtesting results show that the VaR calculated from HMM HAC performs significantly better.

The second application is on modeling a rainfall process. HMM is a conventional model for rainfall data, however, bringing HMM and HAC together for modeling the multivariate rainfall process is an innovative modeling path.

5.1. Application I

5.1.1. Data. The data set consists of the daily values for the exchange rates JPY/EUR, GBP/EUR, and USD/EUR. The covered period is [4.1.1999; 14.8.2009], resulting in 2771 observations.

To eliminate intertemporal conditional heteroscedasticity, we fit a univariate GARCH(1,1) process to each marginal time series of log-returns

$$Y_{j,t} = \mu_{j,t} + \sigma_{j,t}\varepsilon_{j,t} \quad \text{with } \sigma^2_{j,t} = \omega_j + \alpha_j \sigma^2_{j,t-1} + \beta_j (Y_{j,t-1} - \mu_{j,t-1})^2 \tag{24}$$

and $\omega > 0$, $\alpha_j \geq 0$, $\beta_j \geq 0$, $\alpha_j + \beta_j < 1$.

The residuals exhibit the typical behavior: they are not normally distributed, which motivates nonparametric estimation of the margins. From the results of

https://doi.org/10.1017/S0266466614000607 Published online by Cambridge University Press

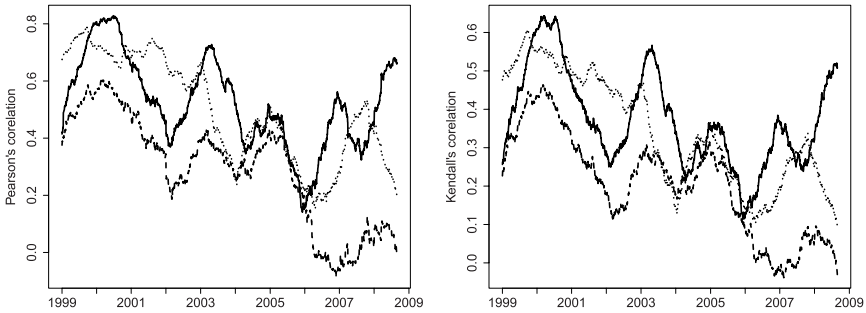

FIGURE 8. Rolling window estimators of Pearson's (left) and Kendall's (right) correlation coefficients between the GARCH(1,1) residuals of exchange rates: JPY and USD (solid line), JPY and GBP (dashed line), GBP and USD (dotted line). The width of the rolling window is set to 250 observations.

the Box–Ljung test, whose p-values are $0.73, 0.01$, and 0.87 for JPY/EUR, GBP/EUR, and USD/EUR, we conclude that the autocorrelation of the residuals is strongly significant only for the GBP/EUR rate. After this intertemporal correction, we work only with the residuals.

The dependency variation is measured by Kendall's and Pearson's correlation coefficients: Figure 8 shows the variation of both coefficients calculated in a rolling window of width $r = 250$. Their dynamic behavior is similar, but not identical. This motivates once more a time varying copula based model.

5.1.2. Fitting a HMM model. Figures 1, 9, and 10 summarize the analysis using three methods: moving window, LCP, and HMM HAC. LCP uses moving windows, with varying sizes. To be more specific, LCP is a scaling technique which determines a local homogeneous window at each time point, see Härdle et al. (2013). In contrast to LCP, HMM HAC is based on a global modeling concept rather than a local one. One observes relatively smooth changes of the parameters, see Figures 1 and 9. HMM HAC is as flexible as LCP, as can be seen from Figures 1, 9, and 10, since the estimated structure also takes three values and is confirmed by the variations of structures estimated from LCP. Moreover, the moving window analysis or LCP can serve as a guideline for choosing the initial values for our HMM HAC. Figure 11 displays the number of states for HMM HAC for rolling windows with a length of 500 observations.

A VaR estimation example is undertaken to show the good performance of HMM HAC. We generate $N = 10^4$ paths with $T = 2219$ observations, and $|W| = 1000$ combinations of different portfolios, where $W = \{(1/3, 1/3, 1/3)^\top \bigcup [\mathbf{w} = (w_1, w_2, w_3)^\top]\}$, with $w_i = w_i' / \sum_{i=1}^3 w_i'$, $w_i' \in U(0, 1)$. The Profit Loss (P&L) function of a weighted portfolio based on assets y_{td} is $L_{t+1} \stackrel{\text{def}}{=} \sum_{d=1}^3 w_i (y_{t+1d} - y_{td})$, with weights $\mathbf{w} = (w_1, w_2, w_3) \in W$. The VaR of a particular portfolio at

https://doi.org/10.1017/S0266466614000607 Published online by Cambridge University Press

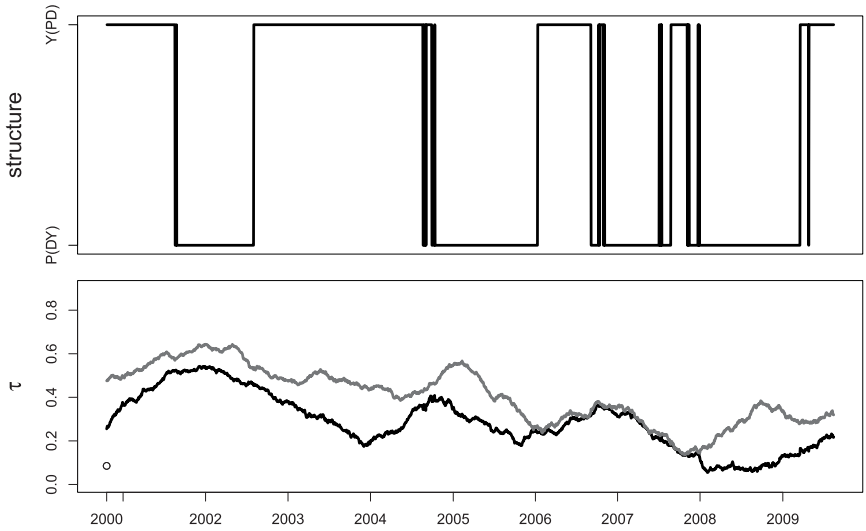

FIGURE 9. Rolling window for exchange rates: structure (upper) and dependency parameters (lower, θ_1 (gray) and θ_2 (black)) for Gumbel HAC. Rolling window size $win = 250$.

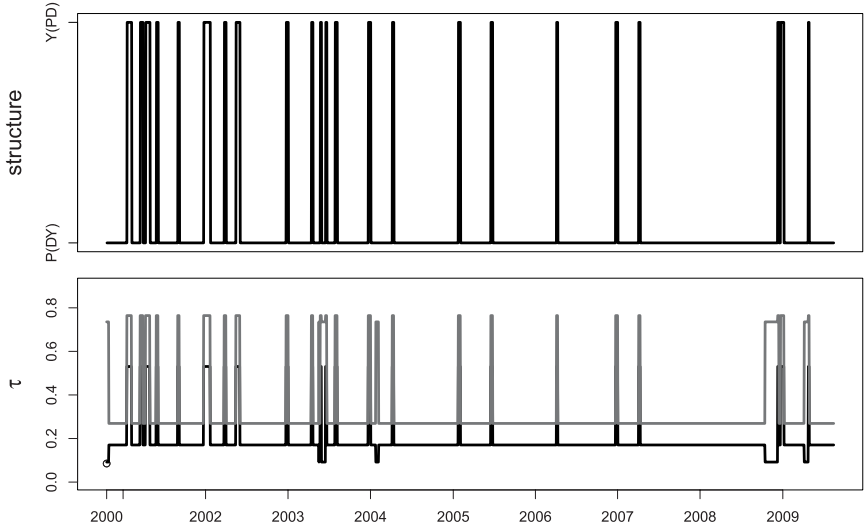

FIGURE 10. HMM for exchange rates: structure (upper) and dependency parameters (lower, θ_1 (gray) and θ_2 (black)) for Gumbel HAC.

https://doi.org/10.1017/S0266466614000607 Published online by Cambridge University Press

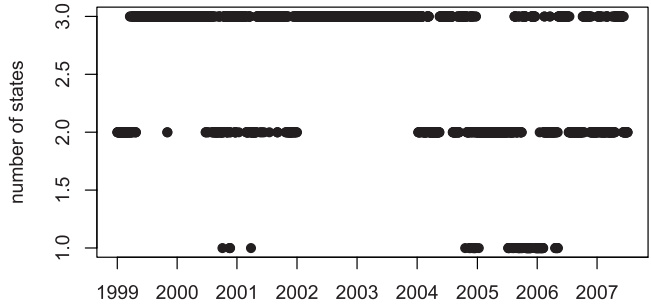

FIGURE 11. Plot of estimated number of states for each window.

level $0 < \alpha < 1$ is defined as $VaR(\alpha) \stackrel{\text{def}}{=} F_L^{-1}(\alpha)$, where the $\hat{\alpha}_{\mathbf{w}}$ is estimated as a relative fraction of violations, see Table 5:

$$\hat{\alpha}_{\mathbf{w}} \stackrel{\text{def}}{=} T^{-1} \sum_{t=1}^{T} \mathbf{I}\{L_t < \widehat{VaR}_t(\alpha)\},$$

and the distance between $\hat{\alpha}_{\mathbf{w}}$ and α is

$$e_{\mathbf{w}} \stackrel{\text{def}}{=} (\hat{\alpha}_{\mathbf{w}} - \alpha)/\alpha.$$

If the portfolio distribution is i.i.d., and a well calibrated model properly mimicks the true underlying asset process, $\hat{\alpha}_{\mathbf{w}}$ is close to its nominal level α. The performance is measured by averaging $\alpha_{\mathbf{w}}$ over all $|W|$ portfolios, see Table 5.

We consider four main models: HMM HAC for 500 observation windows for Gumbel and rotated Gumbel; multiple rolling window with 250 observations windows; LCP with $m_0 = 20$ and $m_0 = 40$ with Gumbel copulae (the LCP finds the optimal length of window in the past by a sequence of tests on windows of increasing sizes, m_0 is a starting window size); and DCC, see Engle (2002), based

TABLE 5. VaR backtesting results, $\bar{\hat{\alpha}}$, where "Gum" denotes the Gumbel copula and "RGum" the rotated survival Gumbel one

	Window\α	0.1	0.05	0.01
HMM, RGum	500	0.0980	**0.0507**	**0.0128**
HMM, Gum	500	**0.0981**	0.0512	0.0135
Rolwin, RGum	250	0.1037	0.0529	0.0151
Rolwin, Gum	250	0.1043	0.0539	0.0162
LCP, $m_0 = 40$	468	0.0973	0.0520	0.0146
LCP, $m_0 = 20$	235	0.1034	0.0537	0.0169
DCC	500	0.0743	0.0393	0.0163

https://doi.org/10.1017/S0266466614000607 Published online by Cambridge University Press

TABLE 6. Robustness relative to $A_W(D_W)$

	Window\α	0.1	0.05	0.01
HMM, RGum	500	−0.0204 (0.013)	**0.0147** (0.012)	**0.2827** (0.064)
HMM, Gum	500	**−0.0191** (0.008)	0.0233 (0.018)	0.3521 (0.029)
Rolwin, RGum	250	0.0375 (0.009)	0.0576 (0.012)	0.5076 (0.074)
Rolwin, Gum	250	0.0426 (0.009)	0.0772 (0.030)	0.6210 (0.043)
LCP, $m_0 = 40$	468	−0.0270 (0.010)	0.0391 (0.018)	0.4553 (0.037)
LCP, $m_0 = 20$	235	0.0344 (0.009)	0.0735 (0.026)	0.6888 (0.050)
DCC	500	−0.2573 (0.015)	−0.2140 (0.015)	0.6346 (0.091)

on 500 observation windows. For each model we make an out of sample forecast. To better evaluate the performance, we calculated the average and SD of e_W:

$$A_W = \frac{1}{|W|}\sum_{\mathbf{w}\in W} e_{\mathbf{w}}, \qquad D_W = \left\{\frac{1}{|W|}\sum_{\mathbf{w}\in W}(e_{\mathbf{w}} - A_W)^2\right\}^{1/2}.$$

Tables 5 and 6 show the backtesting performance for the described models. One concludes that HMM HAC performs better than the concurring moving window, LCP, or DCC, as A_w and D_w are typically smaller in absolute value.

5.2. Application II

Rainfall models are used to forecast, simulate, and price weather derivatives. The difficulty in precipitation data is the nonzero point mass at zero and spatial relationships, see Ailliot, Thompson, and Thomson (2009) for Gaussian dependency among locations with HMM application.

In this application we extend it to a copula framework. Unlike application I, the marginal distribution here vary over states. We propose two methods for modeling the marginal distributions: one is to take y_{tk} to be censored normal distributions, with the following equation:

$$f_k^{\mathrm{m}}\{y_{tk}\} = \begin{cases} 1 - p_k^{x_t} & y_{tk} = 0, \\ p_k^{x_t}\varphi[\{y_{tk} - \mu^{x_t}(k)\}/\{\sigma^{x_t}(k)\}]/\sigma^{x_t}(k) & y_{tk} > 0; \end{cases}$$

with $k = 1, \ldots, d$ as the location, $\varphi(\cdot)$ as the standard normal density, $p_k^{x_t}$ as the rainfall occurrence probability for the location k and state x_t, and $\mu^{x_t}(k), \sigma^{x_t}(k)$ the mean and standard deviation parameters at time t for location k.

A second proposal for the marginal distributions are the gamma distributions:

$$f_k^{\mathrm{m}}\{y_{tk}\} = \begin{cases} 1 - p_k^{x_t} & y_{tk} = 0, \\ p_k^{x_t}\gamma\{y_{tk}; \alpha(k)^{x_t}, \beta(k)^{x_t}\} & y_{tk} > 0; \end{cases}$$

https://doi.org/10.1017/S0266466614000607 Published online by Cambridge University Press

where again the $\alpha(k)^{x_t}, \beta(k)^{x_t}$ are the shape and scale parameters for state x_t and location k. We take the joint distribution function to be a truncated version of a continuous copula function, with the copula density $c_d(\cdot)$ denoted by

$$c_d(\mu,\theta) = \begin{cases} c_c(\mu,\theta), & y_{tk} > 0, \forall k, \\ \partial C_c(\mu,\theta)/\partial\mu_{k_1}\ldots\partial\mu_{k_B}, & k_i \in \{y_{tk_i} > 0\}, i \in 1,\ldots,E; \end{cases} \tag{25}$$

where E denotes the number of wet places among the d locations, the C_c are the continuous copula functions, and c_c are the continuous copula densities.

Assume that the daily rainfall observations from the same month are yearly independent realizations of a common underlying hidden Markov model, whose states represent different weather types. As an example, we take every June's daily rainfall.

$$\begin{aligned} &\log p_T(y_{0:T}, x_{0:T}; \upsilon \times \omega) \\ &\quad = \sum_{i=1}^{M} \mathbf{1}\{x_0 = i\} \log\{\pi_i f_i(y_0)\} + \sum_{t=1}^{T}\sum_{i=1}^{M}\sum_{j=1}^{M} \mathbf{1}\{x_t = j\}\mathbf{1}\{x_{t-1} = i\} \log\{p_{ij} f_j(y_t)\} \\ &\qquad + \sum_{t\in B}\sum_{i=1}^{M} \left[\mathbf{1}\{x_t = i\}\{\log(\pi_i)\} - \sum_{j=1}^{M} \mathbf{1}\{x_t = i\}\mathbf{1}\{x_{t-1} = j\} \log(p_{ji}) \right], \end{aligned}$$

with B is the set of days which are the first day of June for each year. We use here 50 years of rainfall data from three locations in China: Guangxi, Guangdong, and Fujian (Figure 12). The graphical correlation can naturally be captured by the fitting of different copulae state parameters.

Table 7 presents (with a truncated Gumbel) the estimated three states, the corresponding different marginal distributions and copula parameters, with estimated initial probability: $\hat{\pi}_{X_t} = (0.298, 0.660, 0.042)$ and estimated transition probability matrix:

$$\hat{P} = \begin{pmatrix} 0.590 & 0.321 & 0.089 \\ 0.188 & 0.742 & 0.080 \\ 0.329 & 0.271 & 0.400 \end{pmatrix}.$$

In the case of our data, gamma distributions fit better as marginals. The states filtered out represent different weather types. The third states are the most humid states, with high rainfall occurrence probabilities, while the second states are drier, and the first are the driest. From the parameters of the gamma distributions, one sees that the variance increases from the first to the third states, which indicates a higher chance for heavy rainfall for the humid states.

To validate our model, 1000 samples of artificial time series of 1500 observations were generated from the fitted model and compared with the original data. Table 8 presents the true Pearson correlation compared with the estimated ones from the generated time series. The 5% confidence intervals of the estimators cover the true correlation, which implies that the simulated rainfall can describe the real correlation of the data quite well. Figure 13 shows a marginal plot

https://doi.org/10.1017/S0266466614000607 Published online by Cambridge University Press

FIGURE 12. Map of Guangxi, Guangdong, Fujian in China.

TABLE 7. Rainfall occurrence probability and shape, scale parameters estimated from HMM (data 1957–2006)

X_t	Shape	Scale	Occur Prob
1	(0.442, 0.429, 0.552)	(139.33, 116.70, 169.66)	(0.252, 0.256, 0.439)
2	(0.671, 0.618, 0.561)	(273.83, 253.25, 427.46)	(0.806, 0.786, 0.683)
3	(0.636, 1.125, 0.774)	(381.09, 264.83, 514.08)	(0.667, 1.000, 0.944)

TABLE 8. True correlations, simulated averaged correlations from 1000 samples and their 5% confidence intervals. 1 Fujian, 2 Guangdong, 3 Guangxi

Location	True	$\widehat{\text{Corr}}(Y_{t,1}, Y_{t,2})$
1 – –2	0.308	0.300 (0.235, 0.373)
2 – –3	0.261	0.411 (0.256, 0.586)
1 – –3	0.203	0.130 (0.058, 0.215)

of the log survival function derived from the empirical cdf of the real data and generated data. The log survival function is a transformation of the marginal cdf $F_k^{\text{m}}(y_{tk})$:

$$\log\{1 - F_k^{\text{m}}(y_{tk})\}. \tag{26}$$

https://doi.org/10.1017/S0266466614000607 Published online by Cambridge University Press

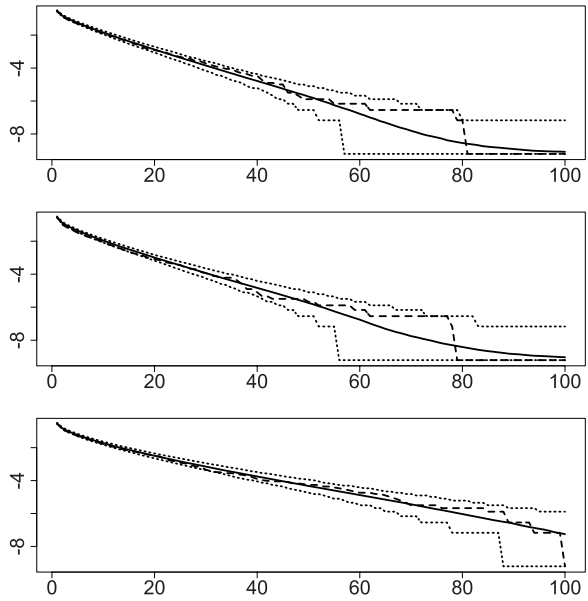

FIGURE 13. Log-survivor-function (black solid) and 95% prediction intervals (gray dotted) of the simulated distribution for the fitted model with sample log-survivor-function superimposed (black dashed).

Again we see that the 95% confidence interval can cover the true curve fairly well.

Table 8 contains the autocorrelations and cross-correlations of the real data and the generated time series. Unfortunately, our generated time series does not show a similar autocorrelation or cross-correlation. Since there is usually more than one significant lag of autocorrelation or cross-correlation, the simulated time series mostly only have one lag. This is an issue also observed in Ailliot et al. (2009). The precipitation can be modeled first by a vector autoregressive (VAR) type model, adjusted for zero observations. An alternative could be to impose an additional dependency structure on $\{Y_t\}$.

6. CONCLUSION

We propose a dynamic model for multivariate time series with non-Gaussian dependency. Applying an HMM for general copulae leads to a rich clan of dynamic dependency structures. The proposed methodology is helpful in studying financial contagion at an extreme level over time, and it can naturally help in deriving conditional risk measures, such as CoVaR, see Adrian and Brunnermeier (2011). We have shown that dynamic copula models fit financial markets well, and rainfall patterns too.

https://doi.org/10.1017/S0266466614000607 Published online by Cambridge University Press

In the financial application, we performed deGARCHing to remove the second order dependencies in the marginal time series. As this is a $\sqrt{n}$ step, it will not contaminate the final estimation, and our simulation study confirms this. In the rainfall application, we extend our model to allow the marginal distribution's parameters to also vary over states. Typically it will adapt to nonstationary marginal time series with trend.

REFERENCES

Adrian, T. & M.K. Brunnermeier (2011) CoVaR, *Staff Reports 348*, Federal Reserve Bank of New York.

Ailliot, P., C. Thompson, & P. Thomson (2009) Space-time modeling of precipitation by using a hidden Markov model and censored Gaussian distributions. *Journal of the Royal Statistical Society* 58, 405–426.

Bickel, P.J., Y. Ritov, & T. Rydén (1998) Asymptotic normality of the maximum-likelihood estimator for general hidden Markov models. *Annals of Statistics* 26(4), 1614–1635.

Bickel, P.J. & M. Rosenblatt (1973) On some global measures of the deviations of density function estimates. *The Annals of Statistics* 1, 1071–1095.

Bradley, R. (1986) Basic properties of strong mixing conditions. In E. Eberlein & M.S. Taqqu (eds.), *Dependence in Probability and Statistics*, pp. 165–192. Birkhauser.

Caia, Z., X. Chen, Y. Fan, & X. Wang (2006) Selection of Copulas with Applications in Finance. Working paper. Available at http://www.economics.smu.edu.sg/femes/2008/papers/219.pdf.

Cappé, O., E. Moulines, & T. Rydén (2005) *Inference in Hidden Markov Models*. Springer-Verlag.

Chen, X. & Y. Fan (2005) Estimation of copula-based semiparametric time series models. *Journal of Econometrics* 130(2), 307–335.

Chen, X. & Y. Fan (2006) Estimation and model selection of semiparametric copula-based multivariate dynamic models under copula misspecification. *Journal of Econometrics* 135, 125–154.

Dempster, A., N. Laird, & D. Rubin (1977) Maximum likelihood from incomplete data via the em algorithm (with discussion). *Journal of the Royal Statistical Society B* 39, 1–38.

Engle, R. (2002) Dynamic conditional correlation. *Journal of Business and Economic Statistics* 20(3), 339–350.

Fuh, C.-D. (2003) SPRT and CUSUM in hidden Markov models. *Annals of Statistics* 31(3), 942–977.

Gao, X. & P.X.-K. Song (2011) Composite likelihood EM algorithm with applications to multivariate hidden Markov model. *Statistica Sinica* 21, 165–185.

Giacomini, E., W.K. Härdle, & V. Spokoiny (2009) Inhomogeneous dependence modeling with time-varying copulae. *Journal of Business and Economic Statistics* 27(2), 224–234.

Hamilton, J. (1989) A new approach to the economic analysis of nonstationary time series and the business cycle. *Econometrica* 57(2), 357–384.

Härdle, W., H. Herwartz, & V. Spokoiny (2003) Time inhomogeneous multiple volatility modeling. *Journal of Financial econometrics* 1(1), 55–95.

Härdle, W.K., O. Okhrin, & Y. Okhrin (2013) Dynamic structured copula models. *Statistics & Risk Modeling* 30(4), 361–388.

Joe, H. (1997) *Multivariate Models and Dependence Concepts*. Chapman & Hall.

Leroux, B.G. (1992) Maximum-likelihood estimation for hidden Markov models. *Stochastic Processes and their Applications* 40, 127–143.

Liu, W. & W. Wu (2010) Simultaneous nonparametric inference of time series. *The Annals of Statistics* 38, 2388–2421.

McLachlan, G. & D. Peel (2000) *Finite Mixture Models*. Wiley.

McNeil, A.J. & J. Nešlehová (2009) Multivariate Archimedean copulas, d-monotone functions and l_1 norm symmetric distributions. *Annals of Statistics* 37(5b), 3059–3097.

Nelsen, R.B. (2006) *An Introduction to Copulas*. Springer-Verlag.
Okhrin, O., Y. Okhrin, & W. Schmid (2013) On the structure and estimation of hierarchical Archimedean copulas. *Journal of Econometrics* 173, 189–204.
Okimoto, T. (2008) Regime switching for dynamic correlations. *Journal of Financial and Quantitative Analysis* 43(3), 787–816.
Patton, A.J. (2004) On the out-of-sample importance of skewness and asymmetric dependence for asset allocation. *Journal of Financial Econometrics* 2, 130–168.
Pelletier, D. (2006) Regime switching for dynamic correlations. *Journal of Econometrics* 131, 445–473.
Rabiner, L.R. (1989) A tutorial on hidden Markov models and selected applications in speech recognition. *Proceedings of IEEE* 77(2), 257–286.
Rodriguez, J.C. (2007) Measuring financial contagion: A copula approach. *Journal of Empirical Finance* 14, 401–423.
Savu, C. & M. Trede (2010) Hierarchical Archimedean copulas. *Quantitative Finance* 10, 295–304.
Sklar, A. (1959) Fonctions dé repartition á n dimension et leurs marges. *Publications de l'Institut de statistique de l'Universit de Paris* 8, 299–231.
Whelan, N. (2004) Sampling from Archimedean copulas. *Quantitative Finance* 4, 339–352.

APPENDIX

A.1. Proof of Theorems 3.1 and 3.2

In the HMM HAC framework, let $\{X_t, t \geq 0\}$ with transition probability matrix $P^{\upsilon,\omega} = [p_{ij}^{\upsilon,\omega}]_{i,j=1,\ldots,M}$ and initial distribution $\pi^{\upsilon,\omega} = \{\pi_i^{\upsilon,\omega}\}_{i=1,\ldots,M}$, where $\{\upsilon,\omega\} \in \{V, \Omega\}$ denotes an element in the parameter space $\{V, \Omega\}$ which parametrizes this model, and q is the number of continuous parameters (note that our parameter space is partly discrete (V) and partly continuous (Ω)). We introduce the event $\{\upsilon,\omega\}$ because Ω correspond to events induced by continuous parameters $\boldsymbol{\theta}, s_j, p_{ij}, \pi_i$. Suppose that $B_{t,j}$ is a real-valued additive component equal to $\sum_{k=0}^{t} Y_{k,j}, j \in 1,\ldots,d$, with $B_t = (B_{t,1}, B_{t,2}, \ldots, B_{t,d})^\top$ and with $Y_k = (Y_{k,1}, Y_{k,2}, \ldots, Y_{k,d})^\top$ a r.v. taking values on $\mathbb{R}^d$. Suppose further that $B_{t,j}$ is adjoined to the chain in such a way that $\{(X_t, B_t), t \geq 0\}$ is a Markov chain on $D \times \mathbb{R}^d$ and

$$\begin{aligned} &\mathrm{P}\{(X_t, B_t) \in A \times (B+b) | (X_{t-1}, B_{t-1}) = (i,b)\} \\ &\quad = \mathrm{P}\{(X_1, B_1) \in A \times B | (X_0, B_0) = (i,0)\} \\ &\quad = \mathrm{P}(i, A \times B) = \sum_{j \in A} \int_{b \in B} p_{ij}^{\upsilon \times \omega} f_j \left\{ b; \boldsymbol{\theta}^{(j)}(\upsilon \times \omega), s^{(j)}(\upsilon \times \omega) \right\} \mu(db), \end{aligned} \tag{A.1}$$

where $B, b \subseteq \mathbb{R}^d$, $A \subseteq D$, $f_j\{b; \boldsymbol{\theta}^{(j)}(\upsilon,\omega), s^{(j)}(\upsilon,\omega)\}$ is the conditional density of Y_t given X_{t-1}, X_t with respect to a σ-finite measure μ on $\mathbb{R}^d$, and $\boldsymbol{\theta}(\upsilon,\omega) \in \Theta, s(\upsilon,\omega) \in S$, $j = 1,\ldots,M$ are the unknown parameters. That is, $\{X_t, t \geq 0\}$ is a Markov chain, given $X_0, X_1, \ldots, X_T$, with $Y_1, \ldots, Y_T$ being independent. In this situation, $\{B_t, t \geq 0\}$ is called a *hidden Markov model* if there is a Markov chain $\{X_t, t \geq 0\}$ such that the process $\{(X_t, B_t), t \geq 0\}$ satisfies (A.1). Note that in (A.1), the usual parameterization $\boldsymbol{\theta}^{(j)}(\upsilon,\omega) = \boldsymbol{\theta}^{(j)}$, and $s^{(j)}(\upsilon,\omega) = s^{(j)}$.

Recall the associated parameter space $\{V, \Omega\}$, where V consists of a set of discrete finite elements and Ω is associated with the parameters $\boldsymbol{\theta}, [p_{ij}]_{i,j}$. Define $\mathbf{s}^*$ and $\boldsymbol{\theta}^*$ associated

https://doi.org/10.1017/S0266466614000607 Published online by Cambridge University Press

with the point $\{\upsilon^0, \omega^0\}$ in the parameter space, as follows.

$$q_T(Y_{0:T}; \upsilon^0, \omega^0) \stackrel{\text{def}}{=} \max_{j \in 0,\ldots,M} p_T(Y_{0:T} | x_1 = j; \upsilon^0, \omega^0) \tag{A.2}$$

$$H(\upsilon^0, \omega^0) \stackrel{\text{def}}{=} \mathsf{E}_{\upsilon^0,\omega^0}\{-\log p(Y_0 | Y_{-1}, Y_{-2}, \ldots; \upsilon^0, \omega^0)\}$$

Here, the $Y_{-1}, \ldots, Y_{-T}$ are a finite number of past values of the process.

$$H(\upsilon^0, \omega^0, \upsilon, \omega) \stackrel{\text{def}}{=} \mathsf{E}_{\upsilon^0,\omega^0}\{\log p_T(Y_{0:T}; \upsilon, \omega)\}$$

THEOREM A.1 (Leroux (1992)). *Under A.1–A.5,*

$$\lim_{T\to\infty} T^{-1} \mathsf{E}_{\upsilon^0,\omega^0}\{\log p_T(Y_{0:T}; \upsilon^0, \omega^0)\} = -H(\upsilon^0, \omega^0)$$

$$\lim_{T\to\infty} T^{-1} \log p_T(Y_{0:T}; \upsilon^0, \omega^0) = -H(\upsilon^0, \omega^0),$$

with probability 1*, under* (υ^0, ω^0)*, and*

$$\lim_{T\to\infty} T^{-1} \mathsf{E}_{\upsilon^0,\omega^0}\{\log p_T(Y_{0:T}; \upsilon, \omega)\} = H(\upsilon^0, \omega^0, \upsilon, \omega)$$

$$\lim_{T\to\infty} T^{-1} \log p_T(Y_{0:T}; \upsilon, \omega) = H(\upsilon^0, \omega^0, \upsilon, \omega),$$

with probability 1*, under* (υ^0, ω^0).

LEMMA A.2. $\forall \upsilon_i, u_j, i, j \in 1, \ldots, M$ *as weights, the difference between M linear combination of states leads to*

$$\sum_{i=1}^{M} \upsilon_i f(y, \boldsymbol{\theta}_{s^{(i)}}, s^{(i)}) \neq \sum_{j=1}^{M} \mu_j f(y, \boldsymbol{\theta}_{s'^{(j)}}, s'^{(j)}). \tag{A.3}$$

Proof. For each $s^{(i)}, i \in 1, \ldots, M$ associated with dependency parameter $\boldsymbol{\theta}_{s^{(i)}} \in \mathbb{R}^d_+$. So

$$\sum_{i=1}^{M} \upsilon_i \delta_{s^{(i)}} \neq \sum_{j=1}^{M} \mu_j \delta_{s'^{(j)}}, a.e. \tag{A.4}$$

implies

$$\sum_{i=1}^{M} \upsilon_i \delta_{s^{(i)}} \delta_{\boldsymbol{\theta}_{s^{(i)}}} \neq \sum_{j=1}^{M} \mu_j \delta_{s'^{(j)}} \delta_{\boldsymbol{\theta}_{s'^{(j)}}}, a.e. \tag{A.5}$$

■

Furthermore, if (A.4), then the corresponding point in the parameter space (υ, ω) leads to $\mathcal{K}(\upsilon^0, \omega^0; \upsilon, \omega)$, and (υ, ω) would not be in the equivalent class of (υ^0, ω^0) as long as the points υ and υ^0 are different as (A.4) (the equivalence class of υ^0 is defined in Leroux (1992)), and the divergence between (υ, ω) and (υ^0, ω^0) is defined as

https://doi.org/10.1017/S0266466614000607 Published online by Cambridge University Press

$\mathcal{K}(\upsilon^0,\omega^0;\upsilon,\omega) \stackrel{\text{def}}{=} H(\upsilon^0,\omega^0,\upsilon^0,\omega^0) - H(\upsilon^0,\omega^0,\upsilon,\omega)$. This is connected with the log likelihood ratio process, and one can prove that if either (A.4) or (A.5), and provided that (A.2) holds, then (A.3) will hold, and so $\mathcal{K}(\upsilon^0,\omega^0;\upsilon,\omega) > 0$. Namely, the divergence can distinguish between points from different equivalent classes.

Next, we study whether plugging in nonparametric estimated margins would affect the consistency results by analyzing the uniform convergence of $\hat{f}_i(y)$.

Recall $\hat{f}_i(y) \stackrel{\text{def}}{=} c\{\hat{F}_1^{\mathfrak{m}}(y_1), \hat{F}_2^{\mathfrak{m}}(y_2), \ldots, \hat{F}_d^{\mathfrak{m}}(y_d), \hat{\boldsymbol{\theta}}^{(i)}, \hat{s}^{(i)}\}\hat{f}_1^{\mathfrak{m}}(y_1)\hat{f}_2^{\mathfrak{m}}(y_2)\cdots\hat{f}_d^{\mathfrak{m}}(y_d)$. We have, according to the uniform consistency of copulae density, for all $t \in 1,\ldots,T$, $i \in 1,\ldots,M$,

$$\max_{s^{(i)}} \sup_{y_{t1},\ldots,y_{td}\in B^d, \boldsymbol{\theta}^{(i)}\in\Theta} \Big| \hat{c}(\hat{F}_1^{\mathfrak{m}}(y_{t1}), \hat{F}_2^{\mathfrak{m}}(y_{t2}), \ldots, \hat{F}_d^{\mathfrak{m}}(y_{td}), \boldsymbol{\theta}^{(i)}, s^{(i)}) - c(F_1^{\mathfrak{m}}(y_{t1}), F_2^{\mathfrak{m}}(y_{t2}), \ldots, F_d^{\mathfrak{m}}(y_{td}), \boldsymbol{\theta}^{(i)}, s^{(i)}) \Big| \tag{A.6}$$

$$\leq \sum_{j=1}^{d} \Big| c(F_{1,\eta_1}^{\mathfrak{m}}(y_{t1}), F_{2,\eta_2}^{\mathfrak{m}}(y_{t2}), \ldots, F_{d,\eta_d}^{\mathfrak{m}}(y_{td}))\{\hat{F}_j^{\mathfrak{m}}(y_{tj}) - F_j^{\mathfrak{m}}(y_{tj})\} \Big|, \tag{A.7}$$

where $F_{j,\eta_j}^{\mathfrak{m}}(\cdot) \stackrel{\text{def}}{=} F_j^{\mathfrak{m}}(\cdot) + \eta_j[F(\cdot) - F_j^{\mathfrak{m}}(\cdot)]$, $\eta_j = [0,1]$, and $F_{j,\eta_j}^{\mathfrak{m}}(\cdot)$ lies in the set of admission functions for $F_j^{\mathfrak{m}}$.

Bickel et al. (1998) states that as $\{X_t\}$ is ergodic, then it follows that $\{Y_t\}$ is also ergodic. It is known that any strictly irreducible and aperiodic Markov chain is β-mixing, Bradley (1986). Then the marginal distribution of $Y_{tm}, m = 1,\ldots,M$ follows a process that is β-mixing with an exponential decay rate, namely $\beta_t = \mathcal{O}\{t^{-b}\}$ for some constant a. The temporal dependence of the marginal univariate time series Y_{tm} is inherited simply from the underlying Markov chain as it is a measurable transformation of X_t. Since $\{Y_t\}$ follows HMM HAC, then the marginal distribution of Y_{tm} follows a process that is β-mixing with decay rate $\beta_t = \mathcal{O}(b^{-t})$ for some constant b. Then it follows from the results of Liu and Wu (2010), under assumptions A1–A5, that the marginal kernel density estimation has a Bickel and Rosenblatt (1973)-type of uniform consistency.

$$\sup_{y\in B} \big|\hat{f}_i^{\mathfrak{m}}(y) - f_i^{\mathfrak{m}}(y)\big| = \mathcal{O}_p(1) \tag{A.8}$$

Also according to Chen and Fan (2005),

$$\sqrt{T} \sup_{y\in B} \big|\hat{F}_m^{\mathfrak{m}}(y) - F_m^{\mathfrak{m}}(y)\big| = \mathcal{O}_p(1). \tag{A.9}$$

Finally, we have

$$\max_{s} \sup_{y_1,\ldots,y_d\in B^d, \boldsymbol{\theta}\in E} \Big| \hat{c}(\hat{F}_1^{\mathfrak{m}}(y_1), \hat{F}_2^{\mathfrak{m}}(y_2), \ldots, \hat{F}_d^{\mathfrak{m}}(y_d), \boldsymbol{\theta}^{(i)}, s^{(i)}) - c(F_1^{\mathfrak{m}}(y_1), F_2^{\mathfrak{m}}(y_2), \ldots, F_d^{\mathfrak{m}}(y_d), \boldsymbol{\theta}^{(i)}, s^{(i)}) \Big| = \mathcal{O}_p(1).$$

Therefore, the multivariate distribution at each state satisfies

$$\sup_{y\in B^d} \big|\hat{f}_j(y) - f_j(y)\big| = \mathcal{O}_p(1),$$

https://doi.org/10.1017/S0266466614000607 Published online by Cambridge University Press

where B, B^d are compact sets. So the plug in estimation does not contaminate the consistency results.

To prove the consistency of our estimation of this parameter, we restate the theorems of consistency in Leroux (1992) for our parameter space. One needs to show that for a discrete subspace V^c which does not contain any point of the equivalence class of υ^0, for $\upsilon \in V^c$ and an arbitrary value of $\omega \in \Omega$, that, with probability 1,

$$\lim_{T\to\infty}\left[\min_{\upsilon\in V^c}\log\sup_{\omega\in\Omega} p_T(Y_{0:T};\upsilon,\omega)-\log p_T\left(Y_{0:T};\upsilon^0,\omega^0\right)\right]\to-\infty. \tag{A.10}$$

This follows directly from Lemma A.2 (the identifiability of the state parameters) and its consequence $\mathcal{K}(\upsilon^0,\omega^0;\upsilon,\omega)>0$. Theorem 3.1 is proved.

To prove Theorem 3.2, note that $\lim_{T\to\infty}\max_{i\in 1,\ldots,M}\mathrm{P}(|\hat{\boldsymbol{\theta}}^{(i)}-\boldsymbol{\theta}^{*(i)}|>\varepsilon|\hat{s}^{(i)}=s^{*(i)})$ is conditioned on the event $\{\hat{s}^{(i)}=s^{*(i)}\}$ which asymptotically holds with probability 1. Therefore it suffices to prove, for any $\hat{s}^{(i)}=s^{(i)}$

$$\lim_{T\to\infty}\min_{i\in 1,\ldots,M}\mathrm{P}\left(|\hat{\boldsymbol{\theta}}^{(i)}-\boldsymbol{\theta}^{*(i)}|>\varepsilon\right)=0. \tag{A.11}$$

To show (A.11), one needs to show that for a (V^c,Ω^c) which does not contain any point of the equivalence class of (υ^0,ω^0), we have, with probability 1,

$$\lim_{T\to\infty}\left\{\log\sup_{\omega\in\Omega^c} p_T(Y_{0:T};\upsilon^0,\omega)-\log p_T\left(Y_{0:T};\upsilon^0,\omega^0\right)\right\}\to-\infty, \tag{A.12}$$

which is implied from the following statement: for any closed subset C of Ω^c, there exists a sequence of open subsets of $\mathcal{O}_{\omega_h}$ with $h=1,\ldots,H$ with $C\subseteq\cup_{h=1}^{H}\mathcal{O}_{\omega_h}$, such that

$$\lim_{T\to\infty}\left\{\max_h\log\sup_{\omega\in\mathcal{O}_{\omega_h}} p_T(Y_{0:T};\upsilon^0,\omega)-\log p_T(Y_{0:T};\upsilon^0,\omega^0)\right\}\to-\infty. \tag{A.13}$$

To prove (A.13), we have the modified definition:

$$H(\upsilon^0,\omega^0,\upsilon^0,\omega;\mathcal{O}_{\omega_h})\stackrel{\mathrm{def}}{=}\lim_T\log\sup_{\omega'\in\omega^0} q_T(Y_{0:T},\upsilon^0,\omega')/T. \tag{A.14}$$

It can be derived that

$$H(\upsilon^0,\omega^0,\upsilon^0,\omega)<H(\upsilon^0,\omega^0,\upsilon^0,\omega^0), \tag{A.15}$$

when (υ^0,ω) and (υ^0,ω^0) do not lie in the same equivalence class. Then (A.15) is a consequence of the identifiability condition A.2, and this leads to: $\exists\varepsilon>0$, T_ε and $\mathcal{O}_\omega$ such that

$$\mathsf{E}\log\sup_{\omega'\in\mathcal{O}_\omega} q_{T_\varepsilon}(\upsilon^0,\omega')/T_\varepsilon<\mathsf{E}\log q_{T_\varepsilon}(\upsilon^0,\omega)/T_\varepsilon+\varepsilon<H(\upsilon^0,\omega^0,\upsilon^0,\omega^0)-\varepsilon.$$

Also because $\log\sup_{\omega'\in\mathcal{O}_\omega} p_T(Y_{0:T},\upsilon^0,\omega')/T$ and $\log\sup_{\omega'\in\mathcal{O}_\omega} q_T(Y_{0:T},\upsilon^0,\omega')/T$ have the same limit value, there exists a constant $\varepsilon>0$,

$$\lim_{T\to\infty}\log\sup_{\omega'\in\mathcal{O}_{\omega_h}} p_T(y_{0:T},\upsilon^0,\omega')/T=H(\upsilon^0,\omega^0,\upsilon^0,\omega;\mathcal{O}_{\omega_h})\le H(\upsilon^0,\omega^0,\upsilon^0,\omega^0)-\varepsilon.$$

Now (A.13) follows.

https://doi.org/10.1017/S0266466614000607 Published online by Cambridge University Press

A.2. Proof of Theorem 3.3

Recall from the last subsection, under A.3,

$$\sup_{y\in B}\left|\hat{f}_i^{\mathfrak{m}}(y)-f_i^{\mathfrak{m}}(y)\right|=\mathcal{O}_p(1) \tag{A.16}$$

$$\sqrt{T}\sup_{y\in B}\left|\hat{F}_m^{\mathfrak{m}}(y)-F_m^{\mathfrak{m}}(y)\right|=\mathcal{O}_p(1). \tag{A.17}$$

Let $U_{tm}\overset{\text{def}}{=}F_m^{\mathfrak{m}}(Y_{tm})$, $\tilde{U}_{tm}\overset{\text{def}}{=}\hat{F}_m^{\mathfrak{m}}(Y_{tm})$, and $\mathbf{U}_t\overset{\text{def}}{=}(U_{t1},\ldots,U_{td})$. Define the log likelihood $L_T(\boldsymbol{\theta})=L_T(\boldsymbol{\theta},\mathbf{U}_{0:T})\overset{\text{def}}{=}\log p_T(y_{0:T})$; in our case, we will work with $L_T(\boldsymbol{\theta},\tilde{\mathbf{U}}_{0:T})$. Relying on the LAN property proved in Bickel et al. (1998), under A.1–A.7, we have

$$\begin{aligned}&L_T(\boldsymbol{\theta}^*+T^{-1/2}\boldsymbol{\theta},\mathbf{U}_{0:T})-L_T(\boldsymbol{\theta}^*,\mathbf{U}_{0:T})\\&\quad=T^{-1/2}\boldsymbol{\theta}^\top\partial L_T(\boldsymbol{\theta}^*)+T^{-1}\boldsymbol{\theta}^\top\partial^2L_T(\boldsymbol{\theta}^*)\boldsymbol{\theta}/2+R_T(\boldsymbol{\theta}),\end{aligned} \tag{A.18}$$

where $R_T(\boldsymbol{\theta})$ tends to zero in probability, uniformly on compact subsets of the parameter space of $\boldsymbol{\theta}$.

Next we need to prove that, uniformly over $\boldsymbol{\theta}$,

$$\begin{aligned}&L_T(\boldsymbol{\theta}^*+T^{-1/2}\boldsymbol{\theta},\mathbf{U}_{0:T})-L_T(\boldsymbol{\theta}^*,\mathbf{U}_{0:T})-L_T(\boldsymbol{\theta}^*+n^{-1/2}\boldsymbol{\theta},\tilde{\mathbf{U}}_{0:T})+L_T(\boldsymbol{\theta}^*,\tilde{\mathbf{U}}_{0:T})\\&\quad-T^{-1/2}\boldsymbol{\theta}^\top\sum_t\sum_m W_m(U_{tm})=\mathcal{O}_p\{R_T(\boldsymbol{\theta})\},\end{aligned}$$

where

$$\begin{aligned}W_m(U_{tm})\overset{\text{def}}{=}&\int_{v_1,\ldots,v_d}\{\mathbf{1}(U_{tm}\le v_m)-v_m\}(\mathsf{E}\,\partial\tilde{a}_t\tilde{b}_m/\partial\boldsymbol{\theta}|_{\boldsymbol{\theta}=\boldsymbol{\theta}^*})\\&\times c\left(v_1,\ldots,v_d,\boldsymbol{\theta}^{*(m)},s^{*(m)}\right)dv_1\cdots dv_d.\end{aligned}$$

$\tilde{a}_t(\cdot)$ and $\tilde{b}_m(\cdot)$ are functions defined later in the proof.

Similarly, we have

$$\begin{aligned}&L_T(\boldsymbol{\theta}^*,\tilde{\mathbf{U}}_{0:T})-L_T(\boldsymbol{\theta}^*,\mathbf{U}_{0:T})\\&\quad=\log\left(\frac{\sum_{x_0=1}^M\cdots\sum_{x_T=1}^M\pi_{x_0}\tilde{f}_{x_0}(y_0)\prod_{t=1}^T p_{x_{t-1}x_t}\tilde{f}_{x_t}(y_t)}{\sum_{x_0=1}^M\cdots\sum_{x_T=1}^M\pi_{x_0}f_{x_0}(y_0)\prod_{t=1}^T p_{x_{t-1}x_t}f_{x_t}(y_t)}\right)\\&\quad=\frac{\sum_{x_0=1}^M\cdots\sum_{x_T=1}^M\pi_{x_0}\tilde{f}_{x_0}(y_0)\prod_{t=1}^T p_{x_{t-1}x_t}\tilde{f}_{x_t}(y_t)}{\sum_{x_0=1}^M\cdots\sum_{x_T=1}^M\pi_{x_0}\prod_{t=1}^T p_{x_{t-1}x_t}f_{x_t}(y_t)}\\&\qquad-\frac{\sum_{x_0=1}^M\cdots\sum_{x_T=1}^M\pi_{x_0}f_{x_0}(y_0)\prod_{t=1}^T p_{x_{t-1}x_t}f_{x_t}(y_t)}{\sum_{x_0=1}^M\cdots\sum_{x_T=1}^M\pi_{x_0}\prod_{t=1}^T p_{x_{t-1}x_t}f_{x_t}(y_t)}+\mathcal{O}_p(1)\\&\quad\overset{\text{def}}{=}\sum_t\sum_{x_0=1}^M\cdots\sum_{x_T=1}^M\tilde{a}_t(\boldsymbol{\theta}^*)\{\tilde{f}_{x_t}(y_t)-f_{x_t}(y_t)\}+\mathcal{O}_p(1),\end{aligned}$$

where $\tilde{a}_{t_0}(\boldsymbol{\theta}^*)=\dfrac{\pi_{x_0}\tilde{f}_{x_0}(y_0)\prod_{t=1}^{t_0}p_{x_{t-1}x_t}\tilde{f}_{x_t}(y_t)\prod_{t=t_0+1}^{T}p_{x_{t-1}x_t}f_{x_t}(y_t)}{\sum_{x_0=1}^M\cdots\sum_{x_T=1}^M\pi_{x_0}f_{x_0}(y_0)\prod_{t=1}^T p_{x_{t-1}x_t}f_{x_t}(y_t)}$.

https://doi.org/10.1017/S0266466614000607 Published online by Cambridge University Press

As

$$\begin{aligned}\tilde{f}_{x_t}(y_t) - f_{x_t}(y_t) &= c\left(\tilde{\mathbf{U}}_{0:T}, \boldsymbol{\theta}^{*(x_t)}, s^{*(x_t)}\right) \prod_{m=1}^{d} f_m^{\mathfrak{m}} - c\left(\mathbf{U}_{0:T}, \boldsymbol{\theta}^{*(x_t)}, s^{*(x_t)}\right) \prod_{j=1}^{d} f_j^{\mathfrak{m}} \\ &= \sum_m c_{u_m}\left\{F_1^{\mathfrak{m}}(y_{1t}), F_2^{\mathfrak{m}}(y_{2t}), \ldots, F_d^{\mathfrak{m}}(y_{dt}), \boldsymbol{\theta}^{*(x_t)}, s^{*(x_t)}\right\} \\ &\quad \times \left\{\hat{F}_m^{\mathfrak{m}}(y_{mt}) - F_m^{\mathfrak{m}}(y_{mt})\right\} \prod_{j=1}^{d} f_j^{\mathfrak{m}} + \mathcal{O}_p(1) \\ &\stackrel{\text{def}}{=} \sum_m \tilde{b}_m(\boldsymbol{\theta}^{(x_t)}) \left\{\hat{F}_m^{\mathfrak{m}}(y_{mt}) - F_m^{\mathfrak{m}}(y_{mt})\right\} + \mathcal{O}_p(1),\end{aligned}$$

where $\tilde{b}_m(\boldsymbol{\theta}^{(x_t)}) \stackrel{\text{def}}{=} c_{u_m}\{F^{\mathfrak{m}}(y_{1t}), F^{\mathfrak{m}}(y_{2t}), \ldots, F^{\mathfrak{m}}(y_{dt}), \boldsymbol{\theta}^{(x_t)}, s^{(x_t)}\} \prod_{j=1}^{d} f_j^{\mathfrak{m}}$, and c_{u_m} denotes the partial derivative of the copulae density w.r.t. u_m.

Then it follows that

$$\begin{aligned}&L_T(\boldsymbol{\theta}^* + T^{-1/2}\boldsymbol{\theta}, \mathbf{U}_{1:T}) - L_T(\boldsymbol{\theta}^*, \mathbf{U}_{1:T}) - L_T(\boldsymbol{\theta}^* + T^{-1/2}\boldsymbol{\theta}, \tilde{\mathbf{U}}_{1:T}) + L_T(\boldsymbol{\theta}^*, \tilde{\mathbf{U}}_{1:T}) \\ &\quad = T^{-1/2}\boldsymbol{\theta}^\top \sum_{x_0=1}^{M} \cdots \sum_{x_T=1}^{M} \sum_t \left[\sum_m \partial \tilde{a}_t \tilde{b}_m / \partial \boldsymbol{\theta}\{\hat{F}^{\mathfrak{m}}(y_{mt}) - F^{\mathfrak{m}}(y_{mt})\}\right] + \mathcal{O}_p(T^{-1/2}) \\ &\quad = T^{-1/2}\boldsymbol{\theta}^\top \sum_t \sum_m W_m(U_{tm}) + \mathcal{O}_p(T^{-1/2})\end{aligned}$$

So, let

$$\begin{aligned}B &\stackrel{\text{def}}{=} \mathsf{E}\{\partial^2 L_T(\boldsymbol{\theta}^*, \mathbf{U}_{1:T})\} \\ A &\stackrel{\text{def}}{=} \left\{\partial L_T(\boldsymbol{\theta}^*, \mathbf{U}_{1:T}) + \sum_t \sum_m W_m(U_{tm})\right\}, \qquad \textbf{(A.19)}\end{aligned}$$

Finally, we have that the estimated $\hat{\boldsymbol{\theta}}$ can be represented by $\hat{\boldsymbol{\theta}} - \boldsymbol{\theta}^* = B^{-1}A + \mathcal{O}_p(T^{-1/2})$ coming from Bickel et al. (1998).

https://doi.org/10.1017/S0266466614000607 Published online by Cambridge University Press